

# Perspectives on Core-Collapse Supernova Theory

Adam Burrows

*Department of Astrophysical Sciences*

*Princeton University*

*Princeton, NJ 08544 USA*

*e-mail: burrows@astro.princeton.edu*

*URL: <http://www.astro.princeton.edu/~burrows>*

(Dated: October 31, 2018)

Core-collapse theory brings together many facets of high-energy and nuclear astrophysics and the numerical arts to present theorists with one of the most important, yet frustrating, astronomical questions: “What is the mechanism of core-collapse supernova explosions?” A review of all the physics and the fifty-year history involved would soon bury the reader in minutiae that could easily obscure the essential elements of the phenomenon, as we understand it today. Moreover, much remains to be discovered and explained, and a complicated review of an unresolved subject in flux could grow stale fast. Therefore, in this paper I describe what I think are various important facts and perspectives that may have escaped the attention of those interested in this puzzle. Furthermore, I attempt to describe the modern theory’s physical underpinnings and briefly summarize the current state of play. In the process, I identify a few myths (as I see them) that have crept into modern discourse. However, there is much more to do and humility in the face of this age-old challenge is clearly the most prudent stance as we seek its eventual resolution.

PACS numbers: 97.60.Bw, 26.30.-k, 25.30.Pt, 26.50.+x, 26.20.-f, 26.30.Ef, 95.85.Ry

## CONTENTS

I. Introduction	1
II. Physical Context of Core-Collapse – Basic Scenario	3
A. Progenitors	3
B. Collapse	4
C. Bounce	4
D. Trapping	5
E. The Problem	6
III. The Current Status of Core-Collapse Simulations	7
IV. Important Features of Supernova Theory	8
A. General Themes	8
1. Eigenvalue Problems	9
2. Simultaneous Accretion and Explosion	10
3. Energetics	11
4. Conditions for Explosion by the Neutrino Mechanism	11
5. Instability to Finite Perturbation	12
B. Persistent Myths	12
V. Conclusions	13
Acknowledgments	14
References	14
Figures	17

## I. INTRODUCTION

Stars are born, they live, and they die. Some, the most massive ( $\gtrsim 8M_{\odot}$ ), die explosively, spawning in the process neutron stars or “stellar-mass” black holes while

littering the interstellar medium with many of the elements of existence. But what is this process by which a star’s multi-million year life is terminated abruptly and violently within seconds, then announced over months via the brilliant optical display that is a supernova explosion? Fifty years of theory, calculation, and observation have not definitively answered that question, though a vivid picture of the mechanism and terminal scenario of the dense core of a massive star is emerging.

The solution to the puzzle of the mechanism of core-collapse supernova (CCSN) explosions involves more than just obtaining simulation explosions on supercomputers. If this weren’t the case, theorists would have solved this poser many times (and have!). Rather, the “solution” involves quantitatively explaining a host of astronomical facts that surround the supernova phenomenon. These include, but are not limited to: 1) the canonical explosion energy of  $\sim 10^{51}$  ergs (defined as one “Bethe”), along with its putative distribution from  $\sim 0.1$  Bethes to  $\sim 10$  Bethes. Explosion energy is potentially a function of progenitor mass, rotation rate, magnetic fields, and metallicity. To date, no one has come close to achieving this central goal; 2) the residual neutron star mass and its distribution as a function of star. This involves more than simply noting that the Chandrasekhar mass ( $M_{Ch}$ ) of  $\sim 1.4 M_{\odot}$  is similar to the gravitational masses of well-measured neutron stars (though this fact is relevant to zeroth-order). The proto-neutron star (PNS) fattens by accretion during the respite before explosion, so the density and angular-momentum pro-

files in the progenitor core, the time of explosion, and the amount of fallback are all determining factors that are intimately tied to the mechanism and its unfolding. The branch map connecting progenitor to either neutron star or stellar-mass black hole final states is a related goal; 3) the nucleosynthetic yields as a function of stellar progenitor. Which stars yield how much of which elements is a combined function of a) the pre-explosion stellar evolution to the “onion-skin” structure of progressively heavier elements as one tunnels in to the central core and b) the explosion itself, which determines the mass cut and the degree of explosive nucleosynthetic reprocessing. The yields of the elements between calcium and the iron peak (inclusive) are particularly sensitive to the explosion process, constituting as they do the inner ejecta; 4) the high average pulsar proper motion speeds. Radio pulsars are the fastest population of stars in the galaxy, with average speeds of  $\sim 350 \text{ km s}^{-1}$ , but ranging beyond  $\sim 1000 \text{ km s}^{-1}$ . Asymmetries in the explosion itself and simple momentum recoil are natural culprits, but we don’t have an explanation for their observed speed spectrum, nor for which progenitors give birth to the low proper-motion subclass of neutron stars bound as accreting X-ray sources to globular clusters; and 5) supernova explosion morphologies and ejecta element spatial distributions. Instabilities and asphericities in the explosion itself are compounded by instabilities during the propagation of the supernova shock wave through the progenitor star and the circumstellar medium to create a debris field that is anything but spherical and neatly nested. Even a qualitative identification of the signatures of the explosion process itself in the density and element distributions of the expanding supernova blast and subsequent supernova remnant (SNR) would be an advance.

The literature on core-collapse supernova theory is vast and entails a fifty-year history of hydrodynamics and shock physics, radiative transfer, nuclear physics (at many junctures), neutrino physics, particle physics, statistical physics and thermodynamics, gravitational physics, and convection theory. The explosion signatures, along with those listed in the previous paragraph, are photon light curves and spectra, neutrino bursts, gravitational wave bursts, and meteoritic and solar-system isotope ratios. Thousands of researchers have at one time or another been engaged, many as careerists. To attempt to summarize or synthesize this literature, even with a focus on the theory of the mechanism, would be a gargantuan undertaking. Moreover, since the fundamental mechanism has not been satisfactorily and quantitatively demonstrated, such an ambitious review might seem premature.

Nevertheless, there have in the past been attempts to review core-collapse explosion theory, and some of these contain useful information and perspectives. All, however, due to the inexorable evolution of the subject as researchers have struggled towards the ultimate goal of

understanding, and due to the vastness of the task, are of limited scope and clearly trapped in time. This is natural. However, for those readers who desire a Cook’s tour in the tradition of a standard, though helpful, review of the various aspects of core-collapse theory, I list here a sampling. Neither the samples, nor the sampling are complete, and many of these papers were not written as reviews. For overall perspectives, I point to Bethe (1988;1990), Janka (2001,2012), Janka et al. (2007), Burrows et al. (1995,2007ab), Herant et al. (1994), Kotake, Sato, & Takahashi (2006), Kotake et al. (2012ab), Burrows (2000), and Mezzacappa (2005). For neutrino microphysics, one can consult Dicus (1972), Bruenn (1985), Burrows, Reddy, & Thompson (2006), Tubbs & Schramm (1975), Freedman, Schramm, & Tubbs (1977), and Langanke & Martinez-Pinedo (2003). For equation of state issues, there are Lamb et al. (1981), Lattimer (1981), and Lattimer & Swesty (1991). For massive star evolution and nucleosynthesis, good sources are Burbidge et al. (1957), Weaver, Zimmerman, & Woosley (1978), Woosley & Weaver (1986,1995), Thielemann, Nomoto, & Hashimoto (1996), Weaver & Woosley (1993), Nomoto et al. (1997), Woosley, Heger, & Weaver (2002), and Heger, Woosley, & Spruit (2005). For the connection with gamma-ray bursts, one can turn to Woosley & Bloom (2006) and for gravitational wave signatures there are Ott (2009), Kotake (2012), Müller et al. (2004), and Müller et al. (2012). There are many papers on the computational issues specific to core collapse, but the papers by Arnett (1966,1967,1977), Imshennik & Nadëzhin (1973), Bowers & Wilson (1982), Bruenn (1985), Mayle & Wilson (1988), Liebendörfer et al. (2001), Liebendörfer, Rampp, Janka, & Mezzacappa (2005), Burrows et al. (2000), Livne et al. (2004,2007), and Swesty & Myra (2009) are collectively educational. Ph.D. theses by R. Mayle, A. Marek, and B. Müller are particularly informative. Classics in the subject, though not particularly comprehensive, include Burbidge et al. (1957), Colgate & Johnson (1960), Hoyle & Fowler (1960,1964), Fowler & Hoyle (1964), Colgate & White (1966), Arnett (1966), LeBlanc & Wilson (1970), Wilson (1971), Mazurek (1974), Sato (1975), Bethe et al. (1979), and Bethe & Wilson (1985).

To this set of “reviews,” and in particular to the list of “classics,” one could add many others. However, anyone well-versed in the papers on the above short list will be well-informed on most of supernova theory, if not completely *au courant*. Nevertheless, there are many facets of theory, and various points of principle (some rather crucial), that have been insufficiently emphasized and articulated in detailed research papers, which of necessity present a given, though sometimes narrow, result. The upshot has been some defocusing of the theory enterprise and the accumulation of various myths that, while understood to be such by most practitioners, have at times confused the uninitiated. With this paper, I highlight an eclectic mix of important topics in core-collapse

supernova theory that I feel have not gotten sufficient “air time.” In the process, some of the central features of modern supernova theory are identified. It is hoped that this collection of excursions, though idiosyncratic, will help sharpen collective understanding of the core issues to be tackled on the way to a complete and credible understanding of the explosion phenomenon.

## II. PHYSICAL CONTEXT OF CORE-COLLAPSE – BASIC SCENARIO

### A. Progenitors

A central facet of a star’s evolution is the steady decrease with time of its core specific entropy. The loss by outward diffusion of the energy generated by nuclear transmutation to progressively heavier elements (for which nucleons are more and more organized in the nucleus) naturally leads to these lower entropies. This may seem counter-intuitive, since core temperature increases during and between burning phases. However, core density also increases, and this increase outpaces the temperature increase needed to maintain burning and, as ash becomes fuel, to ignite the next burning stages. In addition, after the ignition of core carbon burning, the temperatures are sufficient to generate high fluxes of thermal neutrinos. These stream directly out of the core, accelerating core evolution and, in the sense of entropy, its refrigeration. This phase also marks the evolutionary decoupling of the stellar photosphere from the burning core, which then inaugurates its more rapid race to collapse.

Entropy is relevant because it is a measure of randomness. A low value bespeaks organization and electron degeneracy. Hence, stellar evolution leads to white dwarf cores. The more massive stars generate more massive cores, and those more massive than  $\sim 8 M_{\odot}$  achieve the Chandrasekhar mass, at which point such cores are unstable to the dynamical implosion (collapse) that inaugurates the supernova. However, the “Chandrasekhar mass,” and its core density profile when achieved, depend upon the electron fraction ( $Y_e$ ) and entropy profiles. The effective Chandrasekhar mass is not its canonical zero-entropy, uniform- $Y_e$  value of  $1.456(2Y_e)^2 M_{\odot}$ . Entropy and  $Y_e$  profiles are functions of the specific evolutionary paths to instability, in particular the character of convective shell burning and the  $^{12}\text{C}(\alpha, \gamma)^{16}\text{O}$  rate. More massive progenitors evolve more quickly, and, therefore, don’t deentropize as much by neutrino losses before collapse. They have higher entropies, resulting in additional pressure beyond that associated with zero-temperature electron degeneracy to support more mass. Therefore, the core mass necessary to go unstable is increased. Note that electron capture on nuclei alters  $Y_e$ , and the rates of electron capture depend sensitively upon isotope and density.

The result is a “Chandrasekhar mass” that could vary from  $\sim 1.25$  to  $\sim 2.0 M_{\odot}$ , depending upon progenitor mass and evolutionary details (Figure 1). The latter are not necessarily perfectly captured by current models. However, the trend seems roughly to be that more massive progenitors have 1) larger effective Chandrasekhar masses and 2) envelopes in which the mass density decreases more slowly and, hence, that position more mass around the core. Figure 2 shows the core density profiles for various theoretical initial progenitor masses. While most massive-star supernova progenitor cores evolve to iron peak elements and a Chandrasekhar-mass “iron core” at the center of the canonical “onion-skin” structure of progressively lighter elements from the inside out, the least massive progenitors (perhaps with ZAMS<sup>1</sup> masses of  $\sim 8.0$ – $9.0 M_{\odot}$ ) are thought to end up as “O-Ne-Mg” cores (Nomoto & Hashimoto 1988). Such cores might have very tenuous outer envelopes which, given current thinking, might result in underenergetic ( $\sim 10^{50}$  ergs  $\equiv 0.1$  Bethe) neutrino-wind-driven explosions (Burrows 1987; Kitaura et al., 2006; Burrows et al. 2007c). In both circumstances, the ashes from shell burning are responsible for fattening the inner core to the effective Chandrasekhar mass. Importantly, the more massive progenitors have slightly lower central densities and temperatures at collapse. The higher densities of “O-Ne-Mg” cores result in higher electron capture rates, but the higher entropies of the more massive progenitors result in a greater softening of the EOS due to photodissociation<sup>2</sup>. Both processes facilitate the achievement of the Chandrasekhar instability, which once achieved is dynamical<sup>3</sup>. Therefore, in a real sense how the Chandrasekhar instability is achieved is secondary, and collapse proceeds similarly in both cases. Some would distinguish “electron-capture supernovae” as a different species of supernova. However, this is really not justified. The true difference is in the envelope density profile (Figure 2). The lowest-mass massive progenitors have very steep density profiles outside the inner core. These translate into sharply dropping accretion rates onto the proto-neutron star after bounce and before explosion. The dynamical differences and outcomes of “iron-core” or “O-Ne-Mg” collapse are more dependent, therefore, on the different outer core mass and density profiles, where the differences are expected to translate into real differences in explosion energy, kick speeds, residual neutron star masses, and optical displays. Since neither core type contains much thermonuclear fuel, unlike in the Type Ia supernova case of

<sup>1</sup> Zero-Age-Main-Sequence

<sup>2</sup> which decreases the effective  $\gamma$  of the gas below the critical value of  $4/3$

<sup>3</sup> The collapse time to nuclear densities is then no more than  $\sim 350$  milliseconds, whatever the progenitor mass. An approximate characteristic dynamical time is very roughly  $\sim 40 \text{ ms} / \sqrt{\rho_{10}}$ , where  $\rho_{10}$  is in units of  $10^{10} \text{ gm cm}^{-3}$ .

critical carbon-oxygen white dwarfs, burning does not inhibit collapse to nuclear densities ( $\sim 2.6 \times 10^{14} \text{ gm cm}^{-3}$ ). However, the reader should note that, due to carbon and neon shell flashes, stellar evolution simulations up to the edge of collapse are very difficult for the lowest-mass massive stars and only one group has provided a massive-star model below  $9.0 M_{\odot}$  (Nomoto & Hashimoto 1988).

I reiterate that the initial core profiles, along with whatever initial rotation may be present in the core at collapse, must determine the spread in outcomes of collapse. In a very real sense, “progenitor is destiny,” a mapping complicated only by the randomness associated with chaotic turbulence and instability dynamics and with the unknown initial perturbation spectrum imposed by pre-collapse convective burning (Meakin & Arnett 2006, 2007ab). Due to such stochasticity, it is expected that a given progenitor star and structure will give rise to a distribution of outcomes (energies, proto-neutron star masses, kick speeds and directions, etc.), with a “ $\sigma$ ” that remains very much to be determined but that many hope (without yet much justification) will be small. The task before theorists is to determine the progenitor/supernova mapping. On the observational side, Smartt (2009) has recently attempted such a mapping by identifying progenitors in archival data to a handful of core-collapse supernovae. His preliminary finding that no progenitor to a supernova with such archival data is more massive than  $\sim 16 M_{\odot}$  is intriguing, but will need further investigation to confirm or refute.

With this background, core collapse proceeds (in theory) similarly for all progenitors. The inner  $\sim 5000\text{--}10,000$  kilometers is the most relevant. Its dynamical time is less than a second, while that of the rest of the star (with a radius of  $\sim 10^7\text{--}10^9$  km), most of which is comprised of hydrogen and helium, is hours to a day. Therefore, the dynamical inner core is decoupled from the outer shells and it is only when the supernova shock wave reaches them that they too participate in the explosive dynamics, but then only as shocked spectators. The initial core densities and temperatures are  $\sim 6\text{--}15 \times 10^9 \text{ gm cm}^{-3}$  and  $\sim 6\text{--}10 \times 10^9$  Kelvin, respectively. The initial core entropies are  $\sim 0.7\text{--}1.2 k_B/\text{baryon}$ , where  $k_B$  is Boltzmann’s constant, while the entropies in the outer fossil convective silicon and oxygen burning shells jump to  $\sim 2\text{--}5$ . There is a corresponding abrupt decrease in density at these shell boundaries, as well as increases in  $Y_e$ , whose initial core values are  $\sim 0.4\text{--}0.43$ . The outer shells are at lower densities, for which the electron capture rates are low and  $Y_e$  is very near 0.5 (Figure 1). The pressures are dominated by degenerate relativistic electrons, with slight thermal and Coulomb corrections, and for most progenitors most of the baryons are in nuclei near the iron peak. If we are dealing with an “O-Ne-Mg” core, burning on infall will rapidly convert it into an “iron-peak” core. For an iron core, the nuclei are in nuclear statistical equilibrium, which is a Saha equi-

librium predominantly between nucleons in and out of nuclei, alpha particles, and the nuclei. Such a “chemical” equilibrium is described, for a given nuclear model, by temperature ( $T$ ), mass density ( $\rho$ ), and  $Y_e$ .

## B. Collapse

The instability that is collapse occurs because the average adiabatic  $\gamma$  in the core is at or below  $4/3$ . Photodissociation and domination by relativistic electrons guarantee this. As collapse proceeds,  $T$  and  $\rho$  both rise. With the temperature increase, more nucleons evaporate from nuclei. If the number of free nucleons were to rise significantly, since they are non-relativistic ideal gases with a  $\gamma$  of  $5/3$ , collapse would be halted and reversed before nuclear densities were achieved. This was the supposition in the early 1970s. However, as Bethe et al. (1979) and others have shown, the increase in temperature of the nuclei populates excited nuclear states, which represent many degrees of freedom. The upshot is a significant increase in the specific heat and the regulation of the temperature increase, since energy that would otherwise be channeled into kinetic degrees of freedom is redirected in part into these excited states. The result is not only moderation in the temperature increase during collapse, but also in the production of non-relativistic free nucleons, thereby maintaining the domination of the pressure by the relativistic electrons and preserving the nuclei during collapse. The consequence is collapse all the way to nuclear densities, at which point nuclei phase transform into nucleons that at such densities experience strong nuclear repulsion, severely inhibiting further compression.

## C. Bounce

Within less than a millisecond, this stiffening of the equation of state halts and reverses collapse. During collapse, since the central speed and outer core speeds must be zero and low (respectively) the peak collapse speed is achieved in the middle of the collapsing core. Early during collapse, this results in a separation into a subsonic inner core, which collapses almost homologously ( $v \propto r$ ) and as a unit, and a supersonically infalling outer core. The peak speed of the inner shells of the outer core are roughly a constant large fraction of free-fall. Therefore, when the inner core achieves nuclear densities and rebounds, because these two regimes are out of sonic contact, the subsonic inner core bounces as a unit and as a spherical piston into the outer core, which is still collapsing inward, thereby generating a shock wave at the interface (Figure 3). This is the supernova shock in its infancy.

During collapse, increasing density and temperature result in increasing electron capture rates on both nu-



clei and free protons, with the resulting decrease in  $Y_e$ . Current thinking is that capture on nuclei predominates (Langanke & Martinez-Pinedo 2003), but since the “iron peak” shifts with the increase in  $\rho$  and the decrease in  $Y_e$  to higher and higher atomic weights, exotic isotopes, for which we have no data, quickly dominate. However, this uncertainty alters the progress of collapse only slightly, since gravitational free fall bounds collapse speeds, whatever the capture rates. The result is that pre-bounce collapse is universal in character, requiring (after peak speeds have achieved  $\sim 1000 \text{ km s}^{-1}$ ) between  $\sim 150$  and  $\sim 350$  milliseconds to achieve bounce. More importantly, rewinding collapse from bounce yields almost universal trajectories relative to bounce time.

#### D. Trapping

As indicated, electron capture during collapse lowers  $Y_e$ , but it also produces electron-type neutrinos ( $\nu_e$ ) at progressively increasing rates. The average energy of these  $\nu_e$ s increases with density and temperature. Since the cross section for scattering off nuclei by the coherent process (Freedman 1974) increases roughly as the square of neutrino energy and the densities are soaring at a rapid rate, the mean-free-paths for  $\nu_e$ -matter interactions are fast decreasing. When these mean-free-paths become comparable to the scale-height of the matter density or when the outward diffusion speed of the  $\nu_e$ s equals the infall speed, then the  $\nu_e$ s are *trapped* in the flow (Mazurek 1974; Sato 1975). After trapping, electron capture is balanced by  $\nu_e$  capture to establish chemical equilibrium at a given electron lepton fraction.

Since this condition is achieved not long after the central density is  $\sim 10^{11} \text{ gm cm}^{-3}$ , trapping of electron lepton number and  $\nu_e$ s happens before much electron capture has occurred and has a profound effect on collapse and subsequent evolution. Trapping locks electron lepton number, electrons, and  $\nu_e$ s in the core for many seconds, depending on the mass shell. The trapped  $\nu_e$ s are compressed significantly, but at low entropy and conserving lepton fraction. The latter settles near 0.30 (partitioned between electrons [ $\sim 0.25$ ] and  $\nu_e$ s [ $\sim 0.05$ ]), instead of 0.03 (all electrons), which it might have been without trapping. The result is the channeling by compression of a significant fraction of the gravitational energy of collapse into *degenerate*  $\nu_e$ s and electrons, with central chemical potentials and Fermi energies of  $\sim 100$ – $300$  MeV. Hence, trapping is not merely the increase of the  $\nu_e$  optical depth far beyond values of one, but the preservation at high values (not far from the initial value of  $\sim 0.43$ ) of the lepton fraction and electron numbers in the core and the production of a sea of degenerate  $\nu_e$  whose average energy, by dint of compression after trapping, is high. If it weren’t for lepton trapping, the  $\nu_e$ s would be thermal with average energies at bounce of  $\sim 30$  MeV,

optical depths of hundreds, and energy diffusion times of  $\sim 50$ – $100$  milliseconds. Instead, their inner core average energies are  $100$ – $300$  MeV, their optical depth to infinity from the center is  $\geq 10^5$ , and the energy diffusion time out of the core is many seconds. The latter has been boosted by the compressional increase in the average  $\nu_e$  energy, for which the  $\nu_e$ -matter cross sections are much larger than they would otherwise be.

By keeping  $Y_e$  high, trapping thwarts the rapid evaporation of neutrons from the nuclei that would otherwise be too neutron-rich to retain them. Therefore, both the increased specific heat due to excited nuclear states and trapping ensure the survival of the nuclei and the maintenance of the effective  $\gamma$  below  $4/3$  until nuclear densities are achieved. If it weren’t for trapping and excited nuclear states, bounce would occur at sub-nuclear densities, the average core electron neutrino energy would be much lower, and  $\nu_e$ -matter mean-free-paths at bounce would be much longer. The lower bounce densities and longer mean-free-paths would have translated directly into much shorter deleptonization and cooling times for a proto-neutron star. Hence, trapping is centrally important in explaining the long duration of the neutrino burst from SN1987A (Kamioka II – Hirata et al. 1987; IMB – Bionta et al. 1987). Before neutrino trapping was recognized, the energy diffusion time out of the proto-neutron star was thought to be  $\sim 100$  milliseconds, a factor of  $\sim 100$  shorter than observed. Moreover, since the total reservoir of energy radiated is fixed at the gravitational binding energy of a cold neutron star ( $\sim \frac{GM^2}{R} \sim 3 \times 10^{53} \text{ ergs} \equiv 300 \text{ Bethes}$ ), a short duration would have implied a higher average neutrino energy ( $\geq 50$  MeV) than measured by Kamioka ( $\sim 15$  MeV – for the  $\bar{\nu}_e$ s). Therefore, and importantly, the lower measured energy and higher measured duration are direct consequences of electron neutrino (lepton number) trapping, a fact not widely appreciated.

Trapping halts the short-term decrease in  $Y_e$  during collapse, but, as mentioned, there is still a slight decrease to  $\sim 0.25$ – $0.35$ . The magnitude of this decrease is enhanced by inelastic scattering of  $\nu_e$ s off electrons (Mezzacappa & Bruenn 1993abc). Like Compton scattering, the capture-produced  $\nu_e$ s are downscattered in energy and at lower energies their Freedman scattering cross sections are lower. The result is a slightly slower increase in the optical depth during infall, and this results in slightly delayed trapping at lower  $Y_e$ s. The magnitude of the effect is  $\sim 0.02$ – $0.03$ .

The trapped  $Y_e$  sets the mass scale of the homologously-collapsing inner core at approximately the associated Chandrasekhar mass (Yahil 1983; Burrows & Lattimer 1983). Since  $M_{Ch}$  is proportional to  $Y_e^2$ , this is  $\sim 0.5$ – $0.6 M_\odot$ . Therefore, the bounce shock first emerges at the sonic point near  $\sim 0.5$ – $0.6 M_\odot$  ( $\sim 10$ – $20$  km) between the inner core and the outer supersonic mantle in an optically thick region. It then propagates down the

density gradient, entropizing the matter it encounters, dissociating the nuclei into nucleons, and reaching lower  $\nu_e$  optical depths within  $\sim 1$  millisecond. At this point, the copious sea of  $\nu_e$ s, newly-liberated by electron capture via the super-allowed charged-current capture process on newly-liberated protons, “breaks out” in a burst that lasts  $\sim 10$  milliseconds (Figure 4). The luminosity of this electron neutrino breakout burst is within an order-of-magnitude of the total optical output of the observable Universe ( $\sim 3 - 4 \times 10^{53}$  ergs s $^{-1}$ ), and is the first, most distinctive, feature of the supernova neutrino emission process. It is a firm prediction of generic core-collapse supernova theory, and if it doesn’t exist, then much of the supernova theory developed in the last  $\sim 35$  years is wrong.

### E. The Problem

The direct mechanism of explosion posits that this bounce shock continues unabated outward into the star and is the supernova. However, both simple theory and detailed numerical simulations universally indicate that the  $\nu_e$  burst and photodissociation of the infalling nuclei debilitate the shock wave into accretion within  $\sim 5$  milliseconds of bounce. In a very real (though approximate) sense, the subsonic inner core and shocked mantle together execute a coherent harmonic oscillation that is near-critically damped. The shock acts like a black-body absorber of sound (the bounce pressure pulse), and the breakout neutrinos and photodissociation do the rest. The breakout neutrino burst directly saps the shock of energy, while photodissociation by the shock redistributes shock energy from the kinetic component (and, hence, pressure) to pay the nuclear binding energy penalty. Contrary to common lore, photodissociation is not a loss of energy — the energy is still there and could be recovered with recombination. Rather, photodissociation softens the equation of state by lowering the  $\gamma$  and raising the specific heat. The result is a less efficient conversion of infall kinetic energy (whose original source is gravity) into pressure. One should note that if electron capture and neutrino transport are both artificially turned off during and after collapse, but a realistic EOS with photodissociation is employed, the direct mechanism can be shown to work for many of the published progenitor models. However, even then, with  $Y_e$  frozen at its initial value and no neutrino burst or losses, the energy of the explosion is never higher than a few tenths of a Bethe, not accounting for the need to overcome the gravitational binding energy of the rest of the star above a “canonical” neutron star mass cut of  $\sim 1.5 M_\odot$  (Figure 5). Something more is needed.

Therefore, since circa 1980 theorists have been presented with a stalled accretion shock at a radius near  $\sim 100$ – $200$  km and have been trying to revive it. This was

and is an unsatisfactory state of affairs. Supernova rates, O- and B-star death rates, and neutron star birth rates all suggest that most massive stars explode as supernovae and leave neutron stars. The fraction that branch into the stellar-mass black hole channel is unknown. The fraction of times stellar-mass black hole formation is accompanied by a supernova is unknown. If the shock is not revived and continues to accrete, all cores will collapse to black holes. The serious revival mechanisms include the delayed neutrino mechanism (Wilson 1985), magnetohydrodynamic (MHD) bipolar jet production (LeBlanc & Wilson 1970; Bisnovatyi-Kogan et al. 1976; Symbalisty 1984; Burrows et al. 2007d; Takiwaki & Kotake 2011) (requiring very rapid rotation), and the acoustic mechanism (Burrows et al. 2006, 2007b). The spherical delayed neutrino mechanism works only weakly, and then only as a wind (Burrows 1987; Kitaura et al. 2006; Burrows et al. 2007c) for one non-representative progenitor (Nomoto & Hashimoto 1988), but the multi-dimensional variant is considered the frontrunner in the generic progenitor case. However, using the most advanced multi-D numerical codes and incorporating detailed microphysics, no one has yet been able to explain or reproduce any of the five “facts” of core-collapse supernova listed at the beginning of the introduction<sup>4</sup>.

The stalled shock continues to dissociate infalling nuclei into nucleons. Electron capture onto the newly-produced nucleons at densities of  $\sim 10^9 - 10^{10}$  gm cm $^{-3}$  and with temperatures of  $\sim 1.5 - 2.5$  MeV rapidly lowers the post-shock  $Y_e$  to values of  $\sim 0.1$ – $0.2$ , creating the characteristic  $Y_e$  trough seen in all detailed simulations (Figure 6). Due both to electron capture behind the shock and neutrino cooling from the neutrinospheres<sup>5</sup> neutrino and electron-lepton-number losses continue apace. The proto-neutron star becomes more and more bound.

Therefore, the object of current intense investigation is a quasi-static proto-neutron star (Burrows & Lattimer 1986; Figure 7) with a baryon mass of  $\sim 1.2$ – $1.5 M_\odot$  (depending upon progenitor), an initial central density at or above  $\sim 4.0 \times 10^{14}$  gm cm $^{-3}$  and rising, a central temperature of  $\sim 10$  MeV (Figure 8) and rising, an inner core entropy of  $\sim 1$ , and a shocked outer mantle entropy with a peak value ranging near  $\sim 6$ – $15$  (Figure 9), all bounded by an accretion shock wave stalled near  $\sim 100$ – $200$  km. During the delay to explosion, the accretion rate ( $\dot{M}$ ) decreases from  $\sim 1.0$  to  $0.3 M_\odot$  per second (for the most massive progenitors) to from  $\sim 0.4$  to  $0.05 M_\odot$  per second (for the least massive progenitors with iron cores). The associated accretion ram pressure, post-shock elec-

<sup>4</sup> except, perhaps, pulsar kicks: Scheck et al. 2004, 2006; Wongwathanarat et al. 2010; Nordhaus et al. 2011

<sup>5</sup> at average radii of  $\sim 20$ – $60$  km, densities of  $\sim 10^{11}$  to  $\sim 10^{12}$  gm cm $^{-3}$ , and temperatures of  $\sim 4$ – $7$  MeV of all six neutrino types ( $\nu_e$ ,  $\bar{\nu}_e$ ,  $\nu_\mu$ ,  $\bar{\nu}_\mu$ ,  $\nu_\tau$ , and  $\bar{\nu}_\tau$ )

tron capture, and deep gravitational potential well are major impediments to explosion. If there were no accretion, neutrino heating would explode the proto-neutron star mantle immediately. The rate of accretion and its evolution are functions strictly of the progenitor mass density profile just prior to collapse, which is a central determinant of the outcome.

### III. THE CURRENT STATUS OF CORE-COLLAPSE SIMULATIONS

There has been palpable progress in the development of techniques and tools to address the core-collapse problem in the last thirty years, but the current status of the theory for the mechanism and the systematics of core-collapse explosions is ambiguous, if not confusing. Wilson (1985), in a pioneering paper and using a spherical code, obtained a neutrino-driven explosion after a short post-bounce delay, but only if he included a mixing-length algorithm to mimic doubly-diffusive “neutron-finger” instabilities that dredged up heat and thereby enhanced the driving neutrino luminosity and heating in the “gain region” (Bethe & Wilson 1985). The gain region is the region behind the shock in which there is net neutrino heating. Without this boost, he did not obtain explosions. However, Bruenn & Dineva (1996) and Dessart et al. (2006) have shown that such instabilities don’t arise in proto-neutron stars. More recently, Kitauro et al. (2006) and Burrows et al. (2007c) obtained weak 1D (spherical) explosions ( $\sim 10^{50}$  ergs) via a neutrino-driven wind for the lowest mass progenitor in the literature ( $\sim 8.8 M_{\odot}$ ). These are the only models credibly shown to explode in 1D (Mezzacappa et al. 2001). This low explosion energy comports with the inference that the energy of explosion may be an increasing function of progenitor ZAMS mass (Utrobin & Chugai 2009). Moreover, explosion occurred before convective overturn instability could be obvious. This result’s 1D simplicity lends credence to these state-of-the-art simulations using the best physics. However, this progenitor has a uniquely steep density gradient just exterior to the core (and, hence, almost no accretion tamp), and such progenitor density profiles and 1D explosion behavior are seen in no other circumstance. This highlights an important point. There is not just one “core-collapse supernova problem,” but many. The properties of presupernova stars vary and so too will the explosion model. More massive stars are more difficult to explode and at some point probably make black holes (Ugliano et al. 2012; O’Connor & Ott 2011; Fryer et al. 1999).

Shock-imposed negative entropy gradients at bounce, neutrino heating from below, the standing-accretion-shock-instability (“SASI”; Blondin, DeMarino, & Mezzacappa 2003; Foglizzo, Scheck, & Janka 2006), and negative lepton gradients in the inner core all render the

shock-bounded environment of the proto-neutron star unstable and turbulent, severely breaking spherical symmetry in the general case. Indeed, it was shown some time ago that multi-dimensional instabilities obtain and are probably central to the core-collapse supernova mechanism in most cases (Burrows & Fryxell 1992; Herant et al. 1992,1994; Burrows, Hayes & Fryxell 1995; Janka & Müller 1996; Blondin, DeMarino, & Mezzacappa 2003; Fryer & Warren 2002,2004; Foglizzo, Scheck, & Janka 2006). The salient processes in the neutrino heating model may be the enhancement of the neutrino-matter heating efficiency, the turbulent pressure, and the enlargement of the gain region, among others. Neutrino heating in the shocked mantle exterior to the neutrinospheres is probably the foremost driver of convection (Burrows, Dolence, & Murphy 2012; Murphy et al. 2012). This is an unexceptional conclusion, since in the neutrino heating mechanism, it is the driver of explosion and the major source of explosion energy.

Using detailed neutrino transport and 2D hydro, Marek & Janka (2009) observed an explosion of a  $15 M_{\odot}$  progenitor via the turbulent neutrino heating mechanism. However, it seems underpowered ( $\leq 10^{50}$  ergs) for this “average” progenitor, and explosion was not seen for their higher-resolution run. Recently, Müller (2011) and Müller, Janka, & Marek (2012) obtained explosions in 2D of both  $11.2 M_{\odot}$  and  $15 M_{\odot}$  progenitors using state-of-the-art neutrino transport with conformal general relativity (emphasizing the importance of the latter; see also Kuroda, Kotake, & Takiwaki 2012), but the explosion energies were  $\sim 2.5 \times 10^{49}$  and  $\sim 10^{50}$  ergs, respectively, at the end of the calculations. When account is taken of the binding energy of the overlying star (Figure 5) these energies could be negative, potentially undermining these state-of-the-art 2D simulations as viable supernova explosion models. However, the asymptotic energies remain to be determined and it should be acknowledged that these are the best 2D simulations of collapse yet performed. However, as in Marek & Janka (2009), though the hydro was 2D, the transport in the Müller (2011) and Müller, Janka, & Marek (2012) papers was done multiple times in 1D along numerous radial rays. The so-called “ray-by-ray” formalism uses the temperature ( $T$ ), density ( $\rho$ ), and electron fraction ( $Y_e$ ) profiles along a given radial ray to feed a 1D spherical transport calculation, that then provides local heating rates. Since vigorous convection in 2D leads to significant angular variation in  $T$ ,  $\rho$ , and  $Y_e$ , this approach exaggerates the variation in the neutrino heating with angle. Ott et al. (2008), performing the only multi-group, multi-angle neutrino transport calculations ever done in 2D, have shown that the integral nature of transport smoothes out the radiation field much more than the matter fields. This suggests that local neutrino heating rates obtained using the ray-by-ray approach might unphysically correlate with low-order mode shock and matter motions, and could be

pumping them unphysically. This may contribute to the perception that the  $\ell = 1$  dipolar shock oscillation seen in such 2D simulations is essential to the turbulent, multi-D neutrino-driven mechanism.

Burrows et al. (2006, 2007b) performed 2D radiation/hydro multi-group, flux-limited simulations and did not obtain neutrino-driven explosions. Their algorithm was Newtonian and did not include velocity-dependent, general-relativistic, or inelastic scattering terms in the transport. Nevertheless,  $\sim 1$  second after bounce they observed vigorous inner core g-mode oscillations that generated a sound pressure field sufficient to explode the envelope. However, the energy of explosion via this “acoustic” mechanism was very slow to accumulate, reaching only  $\sim 10^{50}$  ergs after more than  $\sim 0.5$  seconds. In addition, Weinberg & Quataert (2008) suggest that the amplitude of these g-mode oscillations could be severely diminished by a non-linear parametric resonance that could bleed energy into very short-wavelength modes, dissipating this g-mode oscillation thermally. Such daughter modes are too small to simulate with current grids, but the weakness of the consequent explosions and the possibility of an important additional damping mechanism make this “acoustic” solution sub-optimal. Moreover, if the neutrino mechanism in any form obtains, it would naturally abort the acoustic mechanism.

Rapid rotation with magnetic fields should naturally lead to vigorous explosions and this MHD mechanism has a long history (LeBlanc & Wilson 1970; Symbalisty 1984; Akiyama et al. 2003; Akiyama & Wheeler 2005). The free energy of differential rotation available at bounce if the progenitor core is rapidly rotating ( $P_i \sim 1 - 2$  seconds)<sup>6</sup> is a potent resource, naturally channeled into bipolar jet-like explosions (Burrows et al. 2007d). Figure 10 portrays such a magnetic explosion. A variant of this mechanism has been suggested for gamma-ray bursts (MacFadyen & Woosley 1999). However, pulsar spin data indicate that the generic progenitor core spin rates must be rather low, and that at most  $\sim 1\%$  of collapses can be via such an MHD mechanism. Hence, MHD-driven explosions can’t be the generic core-collapse supernova channel. However, the neutrino heating mechanism may not be able to provide explosion energies above a few Bethe, and this suggests that the best explanation for the rare energetic “hypernovae” might be MHD power due to very rapidly rotating cores.

There are numerous ambiguities and problems with the current generation of 2D simulations that are not reproducing the core-collapse supernova phenomenon. One symptom (or feature) of the problem in 2D may be the long time to explosion seen by, e.g., Marek & Janka

(2009), Suwa, et al. (2010), Müller, Janka, & Marek (2012), and Burrows et al. (2006). Waiting  $\sim 400 - 1000$  milliseconds to explosion may, certainly in the case of the neutrino-heating mechanism, “waste” the neutrinos emitted in the interval after bounce. However, Nature is not 2D and it could be that an impediment to progress in supernova theory over the last few decades is a lack of access to codes, computers, and resources with which to properly simulate the collapse phenomenon in 3D. This could explain the agonizingly slow march since the 1960’s towards demonstrating a robust mechanism of explosion. The difference in the character of 3D turbulence, with its extra degree of freedom and energy cascade to smaller turbulent scales than are found in 2D, might relax the critical condition for explosion (Burrows & Goshy 1993). Indeed, Murphy & Burrows (2008) have shown that the critical condition is more easily met in 2D than in 1D and, recently, Nordhaus, Burrows, Almgren, & Bell (2010) conducted a similar parameter study comparing 1D, 2D, and 3D and found that going from 2D to 3D could lower the threshold for explosion still more. However, Hanke et al. (2012) have called this conclusion into question. Nevertheless, these developments suggest that it is a few tens of percent easier to explode in 3D than in 1D, and that full 3D simulations, but with competitive multi-group neutrino transport, might be needed to properly address this long-standing problem in computational nuclear astrophysics. Such “heroic” 3D simulations will be very computationally challenging, but are the future (Takiwaki, Kotake, & Suwa 2012).

#### IV. IMPORTANT FEATURES OF SUPERNOVA THEORY

Following my description of the core-collapse scenario and my brief summary of the current status of the numerical theory, I now embark upon discussions of select topics, that though important, are often ignored, assumed, or misrepresented. However, I attempt merely to provide simple, yet useful, insights into basic supernova physics – rigor is not here my goal. In the process, I highlight some of the central themes and myths of core-collapse supernova theory. Since I conduct this survey in lieu of a final resolution of the supernova problem, the reader is encouraged to retain an open mind, and forgiven for retaining a critical one.

##### A. General Themes

Frequently missing in general discussions of core-collapse supernovae is that they are gravitationally-powered. Nuclear burning during explosive nucleosynthesis of the outer mantle after the explosion is well along might contribute at most  $\sim 10\%$  of the blast energy. A full solar mass of oxygen and/or carbon would have to burn

<sup>6</sup> translating into a core rotating with  $\sim 1.5$ - to 4-millisecond periods

to iron peak to yield one Bethe. Given all extant progenitor model profiles, much less than that amount of fuel is close enough to the core to achieve by shock heating sufficient temperatures ( $\geq 4 \times 10^9$  K). Moreover, before explosion, any infalling fuel will be burned uselessly during collapse, and the ashes will be dissociated by the stalled shock and then buried in the core. The neutrino energy emitted from the core and absorbed in the proto-neutron star mantle that is required for the neutrino-powered model has its origin in compressive work on the matter of the core by gravitational forces. The trapped leptons are compressed and the matter is heated to high temperatures and thermal energies, both of which represent stored energy eventually to be radiated. Rotationally-powered and magnetic models ultimately derive their energy from the conversion of gravitational binding energy changes during implosion into rotational kinetic energy (roughly conserving angular momentum), and then into magnetic energy.

One of the characteristics of core-collapse supernovae that distinguishes them from thermonuclear (Type Ia) supernovae is that they leave a residue, the neutron star or black hole. It is not necessary to disassemble and unbound this remnant to infinity, thereby paying a severe gravitational binding energy penalty. Since neutrino radiation renders the PNS more and more bound with time, if explosion were to require complete disassembly to infinity, time would not be on the side of explosion. If fact, core-collapse supernovae would probably not be possible. However, in a fundamental sense, core-collapse supernova involve the transfer of energy from the core to the mantle, leaving the core behind. It is the mantle that is ejected. This mantle may start near  $\sim 100$  km, not the canonical radius of  $\sim 10$  km, and hence is much less bound. All CCSN explosion models are different models for core-mantle energy transfer, be it direct hydrodynamic (core piston), neutrino (mantle heating by core neutrinos), or MHD (mantle B-field amplification, tapping core rotation). One can bury in the residue a binding energy problem that could have gotten progressively worse with time.

It may seem curious that the average thermonuclear supernova has an explosion energy that is similar to that of the average CCSN. However, the energy for the former derives from the burning of a large fraction of something like a Chandrasekhar mass, while an energy bound for the latter might be set in part by the gravitational binding energy of the stellar mantle surrounding a Chandrasekhar mass residue. The core-collapse explosion must eject this bound mantle. Burning yields  $\sim 0.5$  MeV per baryon, and the binding energy of a Chandrasekhar mass is roughly  $m_e c^2$  per electron, where  $m_e$  is the electron mass. The latter obtains due to the fact that the Chandrasekhar mass is defined by the onset of relativity for the majority of its electrons. Since  $Y_e$  is  $\sim 0.5$ , and perhaps 50% of a C/O white dwarf burns to make a Type Ia supernova,

both total energies are very approximately the number of baryons in a Chandrasekhar mass times  $\sim 0.5 \times 0.5$  MeV. This is very approximately one Bethe. The binding energy of the white dwarf core of a massive progenitor and the binding energy of the stellar envelope around it will crudely scale with one another, due to the pseudo-power-law density profile of the latter. Therefore, the energy scales for both thermonuclear and gravitational supernovae explosions (the latter in the sense of a bound) are of comparable magnitude. This argument may be good to a factor of a few, but that it is good at all in a Universe with a much wider potential range of energies is perhaps noteworthy.

## 1. Eigenvalue Problems

There are two important approximate eigenvalue problems associated with core collapse. The first involves the post-bounce, pre-explosion PNS structure, bounded by an accretion shock. The hydrodynamics during this phase is roughly quasistatic, so one can drop the time derivatives to arrive at a set of simultaneous ordinary differential equations for the hydrodynamic profiles interior to the accretion shock. With shock outer boundary conditions, an inner core mass ( $M_c$ ), a given accretion rate ( $\dot{M}$ ), and given core neutrino luminosities ( $L_i$ ), one can convert this into an eigenvalue problem for the radius of the shock ( $R_s$ ). One derives  $R_s$  in terms of the control parameters  $\dot{M}$ ,  $L_i$ , and  $M_c$ , given assumptions about mantle heating due to  $L_i$  and cooling due to electron and positron capture on nucleons. As Burrows & Goshy (1993) showed, there is a critical curve in  $L_i$  versus  $\dot{M}$  space (*ceteris paribus*) above which there are no solutions to this eigenvalue problem. As one increases  $L_i$  for a given  $\dot{M}$ ,  $R_s$  increases, but it can not increase to arbitrary values. At a critical curve  $L_i$ ,  $R_s$  is finite, but above the critical value of  $L_i$  for a given  $\dot{M}$  the steady-state problem does not have a solution. The absence of a solution can be considered an approximate condition for explosion by the neutrino heating mechanism. The subsequent evolution is dynamical, with continued neutrino heating depositing energy to power the explosion and expansion of the gas lowering the temperature (not the entropy!) and, thereby, the cooling rates. Furthermore, as the mantle accelerates into explosion, the matter recombines from nucleons and alpha particles into iron peak nuclei (with  $(Z, A)$  depending upon  $Y_e$ ), thereby “returning” to the expanding matter the nuclear binding energy of the ejecta “lost” to shock photodissociation. These “original” ejecta may not contain more than a few hundredths of a solar mass, but since  $\sim 8$ – $9$  MeV are liberated per baryon, only  $\sim 0.1$  solar masses of ejecta are needed to supply approximately one Bethe to the explosion. Similar critical curves can be derived that include multi-dimensional turbulence in 2D (Murphy & Burrows

2008) and 3D (Nordhaus et al. 2010) and these seem to be lower, facilitating explosion. Figure 11 depicts the debris field of such a 3D explosion. However, the detailed reasons for this dimensional boost are still being studied.

The second eigenvalue problem presents itself after explosion and is the neutrino-driven wind that emerges from the proto-neutron star. An old model (Parker 1958) for the solar wind started by assuming that the plasma above the solar photosphere was in hydrostatic equilibrium and that the energy luminosity due to electron conduction through this atmosphere was constant. Since electron conductivity in a hot plasma depends almost solely on temperature ( $\propto T^{5/2}$ ), one derives temperature as a function of radius ( $T \propto 1/r^{2/7}$ ). Hydrostatic equilibrium of an ideal gas can then be integrated to derive the pressure as a function of radius. What one finds is that around a spherical star the pressure must be finite at infinity! This shows that in order to maintain hydrostatic equilibrium the star must be artificially embedded in a high pressure gas. Since the pressure in the interstellar medium is very low, this atmosphere cannot be stable and it would spontaneously erupt as a wind. The flow would transform into a steady-state outflow, with a sonic point and a supersonic asymptotic speed. Though we now know this particular physical model does not apply to the Sun, these arguments led to the prediction of the existence of the solar wind. The wind mass loss rate would be a function of the driving luminosity, the stellar mass, and details of the heating process. It can be shown that if the derived temperature profile falls off more slowly than  $r^{-1}$ , such an atmosphere is similarly unstable.

The relevance of this scientific parable is that the same arguments can (more legitimately) be applied to the mantle of the PNS. The balance of neutrino heating ( $\propto 1/r^2$ ) and neutrino cooling ( $\propto T^6$ ) yields  $T \propto 1/r^{1/3}$ , with a power-law index less than one. Therefore, without a bounding pressure the PNS atmosphere is unstable to a neutrino-driven wind (Duncan, Shapiro, & Wasserman 1986; Burrows 1987; Burrows, Hayes, & Fryxell 1995). In the core-collapse context this bounding pressure is provided by the accretion ram and, while the shock is stalled, the wind is thwarted. However, after explosion and after the pressure around the PNS has subsided due to the progress of the supernova explosion, a neutrino-driven wind naturally emerges. The eigenvalue problem for  $\dot{M}$  as a function of driving luminosity and PNS mass is easily solved.

Therefore, in the context of the delayed neutrino heating model, the supernova itself is the dynamical transitional state between two quasi-steady-state eigenvalue problems, one accretion and the other a wind. The mechanical power in the wind is lower than the instantaneous power being poured into the early supernova because the absorbing mass and neutrino optical depth ( $\tau_\nu$ ) of the atmosphere above the PNS around the gain region

are much larger than in a tenuous wind. At the onset of explosion, how much larger the absorbing mass and depth are determines how much power is available for explosion. If  $\tau_\nu$  is large when the  $\nu_e$  and  $\bar{\nu}_e$  luminosities are large, their product will be large and the explosion will be robust. The simulated explosions of the 8.8- $M_\odot$  progenitor model of Nomoto & Hashimoto (1988), with the very steep density gradient outside the core, transitioned so quickly into a wind that these model supernovae were effectively wind-powered and had the correspondingly low explosion energy alluded to earlier (Kitaura et al. 2006; Burrows et al. 2007c).

## 2. Simultaneous Accretion and Explosion

When breaking spherical symmetry in the context of the multi-dimensional instabilities seen in modern supernova simulations, a feature (some would say a virtue) of many proposed core-collapse supernova mechanisms is that during the early phases of explosion there can be simultaneous explosion and accretion (Burrows et al. 2007a). Continued accretion onto the PNS from one direction can supplement the energy available to power explosion in another.

The neutrino mechanism, in part powered by accretion luminosity, is a good example. In spherical symmetry, explosion is the “opposite” of accretion, and that source of neutrino driving subsides early after the onset of explosion. However, if the symmetry is broken and a neutrino-driven explosion first occurs in one direction, continued accretion onto the PNS from another direction can help maintain the driving neutrino luminosities. Though such accretion might be restricted to a small quadrant, neutrino emissions are always much more isotropic than matter distributions (Ott et al. 2008), with the result that accretion almost anywhere on a PNS surface leads to emitted neutrinos almost everywhere. In a sense, the same is true for the MHD mechanism, wherein explosion is bipolar along the rotation axis, while the spinning PNS accretes along the equator. Conserving angular momentum, such accretion continues to bring in the kinetic energy of differential motion needed to maintain the magnetic energy and pressure that power the explosion. As long as equatorial accretion continues, the core is an “engine” with a power source. After equatorial accretion ceases and the explosion assumes a more isotropic distribution, the engine subsides, but the supernova (or hypernova) is launched. The acoustic mechanism is the quintessential process that exploits simultaneous accretion on one side, which maintains the driving core g-mode oscillations, to power an explosion in the other direction (Burrows et al. 2006, 2007b).

### 3. Energetics

Determining the energy of a detailed numerical explosion can be more awkward than one might think. Usually limited by the small size of the computational domain (e.g., 5000–20000 km), a successful shock wave encounters this border and perforce stops within hundreds of milliseconds of the start of explosion and long before the explosion energy has asymptoted. For such calculations, neutrino energy deposition is still ongoing, recombination of the nucleons and alphas has not completed, and, importantly, the baryon mass cut between the final PNS and the ejecta is not determined. In fact, the mass cut has never been consistently determined for any detailed numerical core-collapse supernova model. In addition, the explosion must work to unbind the star exterior to the mass cut, and this matter (most of the remaining star) can be bound by a few Bethes (see Figure 5). The larger this binding energy, the stronger the explosion in the core needs to be to achieve a given final ejecta supernova kinetic energy. The large magnitude of this binding energy for the most massive progenitors may be instrumental in either aborting what may have started as a promising supernova, or in ensuring that a black hole, rather than a neutron star, remains. In fact, the large binding energies for matter exterior to a canonical  $1.5 M_{\odot}$  in progenitors that one has in the past thought should supernova and leave neutron stars (such as 20 or 25  $M_{\odot}$  ZAMS stars) suggest that either the core explosion must be very vigorous or that explosions in such stars fizzle. This would be unfortunate, since it is thought that the more massive progenitors are the likely primary sources for the oxygen that we see in abundance in the Universe. However, the relevant outer binding energies are functions not only of progenitor mass, but of modeler. This is yet another indication of the centrality of progenitor models to our understanding of the outcome of collapse.

In the neutrino heating model, one way to achieve higher explosion energies may be to explode early. In the current paradigm, during the delay to explosion the neutrino energy deposited is reradiated and useless. There is no accumulation of energy in the post-shock mantle until the explosion is underway. This suggests that a long delay to explosion may be detrimental, wasting as it does the neutrinos radiated by the core before the explosion commences. However, an early explosion may be correspondingly useful, with perhaps some later fallback. Such an early onset may be easier in 3D (Nordhaus et al. 2010). In addition, and counter-intuitively, both before and at the onset of explosion, the enthalpy fluxes and PNS mantle energies are negative, the latter at times even when the recombination energy is accounted for. For all the viable explosion mechanisms, the supernova does not attain its final energy at the instant of explosive instability, but must be driven after it starts and still needs to overcome the PNS and outer stellar envelope

gravitational binding energies. Currently, no detailed neutrino-driving simulation has come within an order of magnitude of achieving this requirement, except perhaps the singular 8.8- $M_{\odot}$  neutrino-wind-driven model.

### 4. Conditions for Explosion by the Neutrino Mechanism

The neutrino mechanism, legitimately the front-runner in the CCSN mechanism sweepstakes, has engendered much speculation concerning the physical conditions for explosion. In section IV.A.1, I described the critical condition between  $\dot{M}$ ,  $L_i$ , and  $M_c$  that signals instability to explosion. This condition, with corrections to account for multi-D effects, still seems close to capturing the essence of the explosion condition. A detailed perturbation analysis of these steady states to explore the complex eigenfrequencies of the monopolar and low-order pulsational modes, in particular to determine when their imaginary parts change sign, would lend a useful additional perspective (Yamasaki & Yamada 2007).

However, other explosion conditions have been proffered which aid understanding (e.g., Pejcha & Thompson 2012; Burrows 1987; Janka 2001). By and large, all these are roughly equivalent. All sensible conditions must recognize that since the matter interior to the pre-explosion shock is in sonic contact the condition for explosion must be a global one. A local condition, say on the pressure at the shock, has little meaning and can be misleading. It is the entire mantle structure that is exploding. Moreover, the discussion in section IV.A.3 indicates how subtle things might be, with explosion commencing even when various otherwise obvious quantities associated with energy or energy flux are negative.

It should be noted that the gain region interior to the shock, in which neutrino heating outpaces capture cooling, surrounds a net cooling region where cooling dominates. The inner boundary of the cooling region coincides, more or less, with the  $\nu_e$  and  $\bar{\nu}_e$  neutrinospheres. This region gradually sinks in due to energy and lepton loss, steadily sending out rarefaction waves that are partially responsible for undermining the gradual outward progress of the quasi-static shock wave and the growth of the gain region. The larger the gain region and the smaller the cooling region the more likely the mantle is to explode. However, the cooling power generally outstrips net heating and this fact is one of the primary impediments to explosion. If there were no cooling region, or if the cooling power in the cooling region were significantly reduced, neutrino absorption would quite easily lead to explosion. A focussed study on how Nature might accomplish this might bear fruit.

A useful approximate condition for explosion is when the characteristic neutrino heating time in the gain region ( $\tau_H$ ) exceeds the advection time ( $\tau_{adv}$ ) through it (Thompson et al. 2005; Janka 2001). For every set of

definitions of these particular times, and there are a variety of definitions which can vary by factors (Murphy & Burrows 2008), the critical ratio itself should be calibrated using hydro. In any case,  $\tau_{adv}$  can be set equal to  $\Delta r/v_{eff}$ , where  $v_{eff}$  is some effective speed through the gain region that incorporates the sinuous trajectories of Lagrangian particles in multi-D. Quite naturally,  $\tau_{adv}$  is larger in 3D than in 2D, and larger in 2D than in 1D (spherical).  $\tau_{adv}$  can also be written as  $\Delta M/\dot{M}$ , where  $\dot{M}$  is the accretion rate through the shock and  $\Delta M$  is the mass in the gain region.

$\tau_H$  can be defined as the internal energy in the gain region divided by the neutrino heating power. The latter is approximately  $L_{\nu_e}\tau_\nu$ , where, again,  $\tau_\nu$  is the electron neutrino optical depth. Therefore, setting  $\tau_H$  equal to  $\tau_{adv}$  gives us  $L_{\nu_e} \sim (\varepsilon/\tau_\nu)\dot{M}$ , where  $\varepsilon$  is the specific energy in the gain region.  $\varepsilon$  might scale with the escape speed squared ( $v_{esc}^2$ ) at the shock, and this quantity scales with the core mass and the inverse of the shock radius (i.e.,  $v_{esc}^2 \sim 2GM_c/R_s$ ). This rough relation yields a critical  $L_{\nu_e}$  versus  $\dot{M}$  curve with a slope of  $(\varepsilon/\tau_\nu)$ , which itself may be a weak function of  $L_{\nu_e}$ ,  $\dot{M}$ , and  $M_c$  that is better calculated numerically. However, this relation can be recast by noting that  $\tau_\nu \sim \kappa_{\nu_e}\rho\Delta r$ , where  $\kappa_{\nu_e}$  is the electron neutrino absorption opacity and  $\rho$  is some mean mass density in the gain region. The result is

$$L_{\nu_e}(crit) \sim \frac{4\pi G\dot{M}}{\kappa_{\nu_e}} \frac{M_c}{\Delta M} R_s. \quad (1)$$

The actual constant of proportionality will depend upon details. Nevertheless, equation (1) states that the higher the absorptive opacity or the ratio of the mass in the gain region to the core mass the lower the critical luminosity for a given  $\dot{M}$  and  $R_s$ . However, the quantity  $R_s/\Delta M$  varies slowly with the control parameters  $L_{\nu_e}$ ,  $\dot{M}$ , and  $M_c$ , making equation(1) a more direct connection between them that succinctly summarizes the critical condition of Burrows & Goshy (1993). A correction factor to account for multi-D effects could be added in the denominator. Not surprisingly, the critical curve and the  $\tau_H = \tau_{adv}$  condition are roughly equivalent.

## 5. Instability to Finite Perturbation

The stalled accretion shock becomes unstable to outward expansion and explosion when (or near when) the critical  $L_{\nu_e}$ - $\dot{M}$ - $M_c$  condition is met and exceeded. However, it is also unstable to an abrupt, finite jump in its position. If, by some mechanism, the shock were to be jolted suddenly to larger radii, the consequently lower matter temperatures would transiently result in a much lower integrated neutrino cooling rate behind the shock, while the larger radius of the shock would result in a larger gain region. Such a sudden, favorable, and finite shift to more heating and less cooling (and to a lower accretion ram

pressure at the shock) could be irreversible and an explosion might be ignited. However, the magnitude of the necessary finite perturbation is not known. The agency of such a jolt is also not known, but the accretion of density discontinuities in the progenitor at composition and entropy boundaries (such as the inner edges of the silicon- or oxygen-burning shells) is seen in hydrodynamical simulations to result in a quick outward (though modest) excursion in the average shock radius. If the actual density jumps are larger than in the current generation of pre-collapse models, or if there are significant variations in the density or velocity profiles of the post-bounce accreting matter, the necessary finite perturbations may be available. To be sure, this discussion is highly speculative, but the possibility remains intriguing that the mantle shell interior to the stalled shock could be nonlinearly unstable to explosion by large, finite-amplitude perturbations.

## B. Persistent Myths

There are a number of what I would call “myths” that have emerged and persisted, despite compelling physical counter-arguments. To be sure, my list is idiosyncratic and the list of others may be different. One myth is that neutrino transport is more difficult than photon transport, requiring only a specialist’s touch. In fact, non-LTE photon transport, with its multitude of level populations, spectroscopic data, collisional processes, and lines, is much more difficult and challenging than neutrino transport. The latter involves only continuum opacities and emissivities and one rate equation, that for  $Y_e$ , which is coupled only to  $\nu_e$  and  $\bar{\nu}_e$  transport. True, there are six neutrino species and one does require knowledge of neutrino-matter couplings. Also, some astronomers shy away from the nuclear and neutrino realm, and are more interested in the dominant signatures of the Universe – those in photons. However, the physics of neutrino transport is far more straightforward than the physics of atomic and molecular spectroscopy and of the myriad collisional processes in a heterogeneous soup of elements and ions. In addition, the numerical art of photon transport is a rigorous, well-developed, subject with expertise spread around the world, whereas experts in neutrino transport are few and far between.

Another myth is that since  $\sim 3 \times 10^{53}$  ergs of binding energy is emitted during the long-term ( $\sim 10$ -50 second) PNS cooling and deleptonization phase, whereas the average core-collapse supernova involves only  $\sim 10^{51}$  ergs, the CCSN is a less than 1% affair, requiring exquisite precision and numerical care in approaching its theory. In fact, since the  $\nu_e$  and  $\bar{\nu}_e$  absorption optical depths in the gain region are  $\sim 4$ –10% and this is the fraction of the core  $\nu_e$  and  $\bar{\nu}_e$  luminosities absorbed in the mantle, the core-collapse neutrino mechanism is more like a



$\sim 4\text{--}10\%$  affair. Nevertheless, it is often suggested that every detail makes a difference to the overall outcome, as if the mechanism itself hinged upon them. The result has been that minor effects have sometimes been allowed to loom large, often confusing those not intimating involved in the research. Examples are  $\nu\text{--}\bar{\nu}$  annihilation, neutrino-electron scattering, electron capture on infall, neutrino-neutrino oscillations, and the nuclear symmetry energy, to name only a few. This is not to say that all these topics are not to be addressed, nor that the ultimate theory can afford to ignore them. Incorporating the correct physics and performing detailed simulations will certainly be necessary to obtain the correct numbers. However, when the best, most detailed, extant exploding 2D CCSN simulations may not be reproducing observed supernova energies by an order of magnitude perhaps a focus on details at the expense of global understanding is unfounded. Something much more important may be missing.

A more innocuous myth is that a stellar-mass black hole can form directly. In fact, in the context of the collapse of an effective-Chandrasekhar-mass core, the inner homologous core will always rebound into the outer core, generating a shock wave. Interior to this shock wave at its inception and during its early life is only  $\sim 1.2\text{--}1.5 M_{\odot}$  of material and this is not enough for the core collectively to experience the general-relativistic instability that leads to stellar-mass black holes. Importantly, the inner core and shocked mantle are out of sonic contact with the supersonically infalling outer core, and, hence, do not yet “know” whether enough mass will accumulate to transition to a black hole. Sufficient matter must accrete through the shock before the core can go unstable. The wait, during which the core will fatten, might require hundreds of milliseconds to seconds. After which a second dynamical collapse to a black hole will ensue. Therefore, black hole formation is always preceded by an intermediate PNS stage and cannot proceed directly (Burrows 1984; Sumiyoshi, Yamada, & Suzuki 2007ab; Fischer et al. 2009; O’Connor & Ott 2011).

Neutrino heating in the gain region naturally generates a negative entropy gradient in the steady state. This gradient is unstable to convective overturn (the generalized Rayleigh-Taylor instability) and leads to turbulence. This turbulence and the corresponding aspherical flow patterns, with neutrino-driven upflowing plumes and associated downflows, has been seen in multi-D simulations since the 1990’s and are central features of supernova theory.

Later, Blondin, Mezzacappa, & DeMarino (2003) identified an instability of the stalled shock, the standing accretion shock instability (“SASI”), that has been well-diagnosed and studied by Foglizzo (2002,2009), Blondin & Mezzacappa (2006), Foglizzo, Scheck, & Janka (2006), Foglizzo et al. (2007), Yamasaki & Foglizzo (2008), Scheck et al. (2008), Iwakami et al. (2008), Kotake et al.

(2009), and Foglizzo et al. (2012). In axisymmetric (2D) studies of the pure SASI (without neutrinos), many witnessed a vigorous dipolar ( $\ell = 1$ ) “sloshing” mode that superficially seems like the corresponding sloshing motion seen in full 2D radiation/hydro simulations. This has led many, I believe incorrectly, to associate the motion seen in most full neutrino-transport runs with the motions seen in the simplified neutrino-free studies. Moreover, since the energy cascade in 2D turbulence (neutrino-driven or otherwise) is “backwards” (Boffetta & Musacchio 2012), from small to large scales, and the SASI instability, by its nature, is on large scales (small spherical harmonic index  $\ell$ ), this chance correspondence of dominant scales in 2D may also in part explain the confusion. More importantly, preliminary calculations performed in 3D (e.g., Burrows, Dolence, & Murphy 2012; Dolence, Burrows, & Murphy 2012; Hanke et al. 2012) do not show the “sloshing” dipolar motion along an axis many have come to associate with the SASI and that some have suggested is crucial to the CCSN mechanism (e.g., Marek & Janka 2009; Hanke et al. 2012). What are seen are bubble structures and plumes indicative of buoyant convection (Figure 12). Hence, the prominent  $\ell = 1$  “SASI” mode may be an artifact of 2D and its inverse cascade. However, when 3D simulations with reasonable physics become more readily available, the fact that the cascade in 3D is in the opposite direction, but the dominant SASI modes are still on large scales, should help clarify the true nature of the turbulence seen.

I include this discussion on the SASI under “myths” because 1) current 3D simulations do not show the signature features of the SASI ostensibly seen in 2D, and 2) I fully expect that when credible and self-consistent 3D radiation/hydrodynamic simulations are performed an objective analysis of its role will reveal it often to be subordinate to neutrino-heated buoyant bubble convection. The reader is cautioned that not every supernova researcher will agree with this characterization, so caveat lector. Nevertheless, and curiously, though simulations with neutrino transport almost always show the classic rising bubble and downflow patterns of buoyancy-driven non-linear convection, many people, even practitioners, had started to refer to all turbulent motions behind the shock as the “SASI.” This may have served to confuse both insiders and outsiders alike. In summary, I am led to suggest that if neutrino driving is the energetic agency of explosion, it is naturally also the primary agency of the turbulence that aids explosion.

## V. CONCLUSIONS

I have sought in this short review of core-collapse supernova theory to clarify its major facets, lay bear its physical underpinnings, and briefly summarize its current status, as I see it. Furthermore, I have tried to identify

some of what I consider to be myths that have crept into theoretical discourse. However, this colloquium is a personal view of the theoretical landscape. There is clearly much more to be done before a cogent explanation of this central astrophysical phenomenon is available and verified, and some of what I have suggested here may not survive future scrutiny. Nevertheless, it is hoped that at the very least this paper provides some novel and useful insights into the physics and astrophysics of both core collapse and supernova explosions.

## ACKNOWLEDGMENTS

The author acknowledges fruitful collaborations with, conversations with, or input from Josh Dolence, Jeremiah Murphy, Christian Ott, Jeremy Goodman, Louis Howell, Rodrigo Fernandez, Manou Rantsiou, Tim Brandt, Eli Livne, Luc Dessart, Todd Thompson, Rolf Walder, Stan Woosley, Ann Almgren, John Bell, and Thomas Janka. He would also like to thank Hank Childs and the VACET/VisIt Visualization team(s) and Mike Chupa of PICSciE for help with graphics and with develop-

ing multi-dimensional analysis tools. A.B. is supported by the Scientific Discovery through Advanced Computing (SciDAC) program of the DOE, under grant number DE-FG02-08ER41544, the NSF under the subaward no. ND201387 to the Joint Institute for Nuclear Astrophysics (JINA, NSF PHY-0822648), and the NSF PetaApps program, under award OCI-0905046 via a subaward no. 44592 from Louisiana State University to Princeton University. Some of the author's science employed computational resources provided by the TIGRESS high performance computer center at Princeton University, which is jointly supported by the Princeton Institute for Computational Science and Engineering (PICSciE) and the Princeton University Office of Information Technology; by the National Energy Research Scientific Computing Center (NERSC), which is supported by the Office of Science of the US Department of Energy under contract DE-AC03-76SF00098; and on the Kraken supercomputer, hosted at NICS and provided by the National Science Foundation through the TeraGrid Advanced Support Program under grant number TG-AST100001.

## REFERENCES

- Akiyama, S., J.C. Wheeler, D.L. Meier, & I. Lichtenstadt, 2003, *Astrophys. J.* **584**, 954.  
Akiyama, S. & J.C. Wheeler, 2005, *Astrophys. J.* **629**, 414.  
Arnett, W.D., 1966, *Canadian Journal of Physics* **44**, 2553.  
Arnett, W.D., 1967, *Can. J. Phys.* **45**, 1621.  
Arnett, W. D., 1977, *Astrophys. J.* **218**, 815.  
Bethe, H. A., G.E. Brown, J. Applegate, & J.M. Lattimer, 1979, *Nucl. Phys. A* **324**, 487.  
Bethe, H. A. & J.R. Wilson, 1985, *Astrophys. J.* **295**, 14.  
Bethe, H. A., 1988, *Ann. Rev. Nucl. Part. Sci.* **38**, 1.  
Bethe, H.A., 1990, *Rev. Mod. Phys.* **62**, 801.  
Bionta, R.M., G. Blewitt, C.B. Bratton, & D. Casper et al. 1987, *Phys. Rev. Lett.* **58**, 1494.  
Bisnovatyi-Kogan, G.S., I.P. Popov, & A.A. Samokhin, 1976, *Astrophys. & Space Sci.* **41**, 287.  
Blondin, J.M., A. Mezzacappa, & C. DeMarino, 2003, *Astrophys. J.* **584**, 971.  
Blondin, J.M. & A. Mezzacappa, 2006, *Astrophys. J.* **642**, 401.  
Boffetta, G. & S. Musacchio, 2012, *Phys. Rev. E* **82**, 016307.  
Bowers, R. L. & J.R. Wilson, 1982, *Astrophys. J. Suppl.* **50**, 115.  
Bruenn, S.W., 1985, *Astrophys. J. Suppl.* **58**, 771.  
Bruenn, S.W. & T. Dineva, 1996, *Astrophys. J.* **458**, L71.  
Burbidge, E., G. Burbidge, W. Fowler, & F. Hoyle, 1957, *Rev. Mod. Phys.* **29**, 547.  
Burrows, A. & J.M. Lattimer, 1983, *Astrophys. J.* **270**, 735.  
Burrows, A., 1984, *Astrophys. J.* **283**, 848.  
Burrows, A. & J.M. Lattimer, 1986, *Astrophys. J.* **307**, 178.  
Burrows, A.i, 1987, *Astrophys. J.* **318**, L57.  
Burrows, A. & B.A. Fryxell, 1992, *Science* **258**, 430.  
Burrows, A. & J. Goshy, 1993, *Astrophys. J.* **416**, 75.  
Burrows, A., J. Hayes, B.A. & Fryxell, 1995, *Astrophys. J.* **450**, 830.  
Burrows, A., 2000, *Nature* **403**, 727.  
Burrows, A., T. Young, P. Pinto, R. Eastman, & T.A. Thompson, 2000, *Astrophys. J.* **539**, 865.  
Burrows, A., S. Reddy, & T.A. Thompson, 2006, *Nuclear Physics A* **777**, 356.  
Burrows, A., E. Livne, L. Dessart, C.D. Ott, & J.W. Murphy, 2006, *Astrophys. J.* **640**, 878.  
Burrows, A., L. Dessart, C.D. Ott, & E. Livne, 2007a, *Phys. Repts.* **442**, 23.  
Burrows, A., E. Livne, L. Dessart, C.D. Ott, & J.W. Murphy, 2007b, *Astrophys. J.* **655**, 416.  
Burrows, A., L. Dessart, & E. Livne, 2007c, in *AIP Conference Series*, ed. S. Immler & R. McCray, Vol. 937, 370.  
Burrows, A., L. Dessart, E. Livne, C.D. Ott, & J.W. Murphy, 2007d, *Astrophys. J.* **664**, 416.  
Burrows, A., J.C. Dolence, & J.W. Murphy, 2012, accepted to *Astrophys. J.* (arXiv:1204.3088).

- Colgate, S.A. & H. J. Johnson, 1960, *Phys. Rev. Lett.* **5**, 235.
- Colgate, S.A. & R.H. White, 1966, *Astrophys. J.* **143**, 626.
- Dessart, L., A. Burrows, E. Livne, & C.D. Ott, 2006, *Astrophys. J.* **645**, 534.
- Dicus, D. 1972, *Phys. Rev. D.* **6**, 941.
- Dolence, J., A. Burrows, & J.W. Murphy, 2012, submitted to *Astrophys. J.* .
- Duncan, R.C., S.L. Shapiro, & I. Wasserman, 1986, *Astrophys. J.* **309**, 141.
- Fischer, T. S.C. Whitehouse, A. Mezzacappa, F.-K. Thielemann, & M. Liebendörfer, 2009, *Astron. Astrophys.* **499**, 1.
- Foglizzo, T., 2002, *Astron. Astrophys.* **392**, 353.
- Foglizzo, T., L. Scheck, & H.-T. Janka, 2006, *Astrophys. J.* **652**, 1436.
- Foglizzo, T., P. Galletti, L. Scheck, & H.-T. Janka, 2007, *Astrophys. J.* **654**, 1006.
- Foglizzo, T., 2009, *Astrophys. J.* **694**, 820.
- Foglizzo, T., F. Masset, J. Guilet, & G. Durand, 2012, *Phys. Rev. Lett.* **108**, 051103.
- Fowler, W.A. & F. Hoyle, 1964, *Astrophys. J. Suppl.* **91**, 201.
- Freedman, D.Z., 1974, *Phys. Rev. D* **9**, 1389.
- Freedman, D.Z., D.N. Schramm, & D.L. Tubbs, 1977, *Ann. Rev. Nucl. Sci.* **27**, 167.
- Fryer, C., S. Woosley, & D. Hartmann, 1999, *Astrophys. J.* **526**, 152.
- Fryer, C.L. & M.S. Warren, 2002, *Astrophys. J. Lett.* **574**, L65.
- Fryer, C.L. & M.S. Warren, 2004, *Astrophys. J.* **601**, 391.
- Hanke, F., A. Marek, B. Müller, & H.-T. Janka, 2012, accepted to *Astrophys. J.* , arXiv:1108.4355.
- Heger, A., S.E. Woosley, & H. Spruit, 2005, *Astrophys. J.* **626**, 350.
- Herant, M., W. Benz, & S.A. Colgate, 1992, *Astrophys. J.* **395**, 642.
- Herant, M., W. Benz, W.R. Hix, C.L. Fryer, & S.A. Colgate, 1994, *Astrophys. J.* **435**, 339.
- Hirata, K. et al., 1987, *Phys. Rev. Lett.* **58**, 1490.
- Hoyle, F. & W.A. Fowler, 1960, *Astrophys. J.* **132**, 565.
- Hoyle, F. & W.A. Fowler, 1964, *Astrophys. J. Suppl.* **9**, 201.
- Imshennik, V. S. & D. K. Nadëzhin, 1973, *Sov. Phys. JETP* **36**, 821.
- Iwakami, W., K. Kotake, N. Ohnishi, S. Yamada, & K. Sawada, 2008, *Astrophys. J.* **678**, 1207.
- Janka, H.-T. & E. Müller, 1996, *Astron. Astrophys.* **306**, 167.
- Janka, H.-T., 2001, *Astron. Astrophys.* **368**, 527.
- Janka, H.-T., K. Langanke, A. Marek, G. Martínez-Pinedo, & B. Müller, 2007, *Phys. Repts.* **442**, 38.
- Janka, H.-T., 2012, accepted to *Ann. Rev. Nucl. Part. Sci.*, (arXiv:1206.2503).
- Kitaura, F.S., H.-T. Janka, & W. Hillebrandt, 2006, *Astron. Astrophys.* **450**, 345.
- Kotake, K., K. Sato, & K. Takahashi, 2006, *Rep. Prog. Phys.* **69**, 971.
- Kotake, K., W. Iwakami, N. Ohnishi, & S. Yamada, 2009, *Astrophys. J. Lett.* **697**, L133.
- Kotake, K., 2012, to appear in a special issue of *Comptes Rendus Physique* “Gravitational Waves (from detectors to astrophysics),” arXiv:1110.5107. [astro-ph]
- Kotake, K. et al., 2012a, accepted in “Advances in Astronomy,” arXiv:1204.2330
- Kotake, K., K. Sumiyoshi, S. Yamada, T. Takiwaki, T. Kuroda, Y. Suwa, & H. Nagakura 2012b, arXiv:1205.6284
- Kuroda, T., K. Kotake, & T. Takiwaki, 2012, *Astrophys. J.* **755**, 11.
- Lamb, D.Q., J.M. Lattimer, C.J. Pethick, & G. Ravenhall, 1981, *Nucl. Phys.* **A360**, 459.
- Langanke, K. & G. Martínez-Pinedo, 2003, *Rev. Mod. Phys.* **75**, 819.
- Lattimer, J. M., 1981, *Ann. Rev. Nucl. Part. Sci.* **31**, 337.
- Lattimer, J.M. & F.D. Swesty, 1991, *Nucl. Phys. A* **535**, 331.
- LeBlanc, J.M. & J.R. Wilson, 1970, *Astrophys. J.* **161**, 541.
- Liebendörfer, M., 2001, Ph.D. thesis (Univ. of Basel).
- Liebendörfer, M., A. Mezzacappa, F.-K. Thielemann, O.E.B. Messer, W.R. Hix, & S.W. Bruenn, 2001, *Phys. Rev. D* **63**, 103004.
- Liebendörfer, M., M. Rampp, H.-T. Janka, & A. Mezzacappa, 2005, *Astrophys. J.* **620**, 840.
- Livne, E., A. Burrows, R. Walder, I. Lichtenstadt, & T.A. Thompson, 2004, *Astrophys. J.* **609**, 277.
- Livne, E., L. Dessart, A. Burrows, & C.A. Meakin, 2007, *Astrophys. J. Suppl.* **170**, 187.
- MacFadyen, A.I. & S.E. Woosley, 1999, *Astrophys. J.* **524**, 262.
- Marek, A., 2006, Ph.D. thesis (Technical Univ., München).
- Marek, A. & H.-T. Janka, 2009, *Astrophys. J.* **694**, 664.
- Mayle, R., 1985, Ph.D. thesis (Univ. of California, Berkeley).
- Mayle, R. & J.R. Wilson, 1988, *Astrophys. J.* , **334**, 909.
- Mazurek, T.J., 1974, *Nature* **252**, 287.
- Meakin, C.A. & D. Arnett, D., 2006, *Astrophys. J. Lett.* **637**, L53.
- Meakin, C. A., & D. Arnett, 2007a, *Astrophys. J.* **665**, 690.
- , 2007b, *Astrophys. J.* **667**, 448.
- Mezzacappa, A. & S.W. Bruenn, 1993a, *Astrophys. J.* **405**, 669.
- , 1993b, *Astrophys. J.* **410**, 740.
- , 1993c, *Astrophys. J.* **405**, 637.
- Mezzacappa, A., M. Liebendörfer, O.E.B. Messer, W.R. Hix, F.-K. Thielemann, & S.W. Bruenn, 2001, *Phys. Rev. Lett.* **86**, 1935.

- Mezzacappa, A., 2005, *Ann. Rev. Nucl. Part. Sci.* **55**, 467.
- Müller, E., M. Rampp, R. Buras, H.-T. Janka, & D.H. Shoemaker, 2004, *Astrophys. J.* **603**, 221.
- Müller, B., 2011, Ph.D. thesis (Technical Univ, München).
- Müller, B., H.-T. Janka, & A. Marek, A., 2012, submitted to *Astrophys. J.* (arXiv:1202.0815).
- Müller, E., H.-T. Janka, & A. Wongwathanarat, 2012, *Astron. Astrophys.* **537**, A63.
- Murphy, J.W. & A. Burrows, 2008, *Astrophys. J.* **688**, 1159.
- Murphy, J.W., J.C. Dolence, & A. Burrows, 2012, submitted to *Astrophys. J.* (arXiv:1205.3491).
- Nomoto, K. & M.A. Hashimoto, 1988, *Phys. Repts.* **163**, 13.
- Nomoto, K., M. Hashimoto, T. Tsujimoto, F.-K. Thielemann, N. Kishimoto, Y. Kubo, & N. Nakasato, 1997, *Nucl. Phys. A* **616**, 79.
- Nordhaus, J., A. Burrows, A. Almgren, & J.B. Bell, 2010, *Astrophys. J.* **720**, 694.
- Nordhaus, J., T. Brandt, A. Burrows, E. Livne, & C.D. Ott, 2011, *Phys. Rev. D* **82**, 103016.
- O’Conner, E. & C.D. Ott, 2011, *Astrophys. J.* **730**, 70.
- Ott, C. D., A. Burrows, L. Dessart, & E. Livne, 2008, *Astrophys. J.* **685**, 1069.
- Ott, C.D., 2009, *Class. Quant. Grav.* **26**, 063001.
- Parker, E., 1958, *Astrophys. J.* **117**, 431.
- Pejcha, O. & T.A. Thompson 2012, *Astrophys. J.* **746**, 106.
- Sato, K., 1975, *Prog. Theor. Phys.* **54**, 1325.
- Scheck, L., T. Plewa, H.-T. Janka, K. Kifonidis, & E. Müller, 2004, *Phys. Rev. Lett.* **92**, 011103.
- Scheck, L., K. Kifonidis, H.-T. Janka, & E. Müller, 2006, *Astron. Astrophys.* **457**, 963.
- Scheck, L., H.-T. Janka, T. Foglizzo, & K. Kifonidis, 2008, *Astron. Astrophys.* **477**, 931.
- Smartt, S., 2009, *Ann. Rev. Astron. & Astrophys.* **47**, 63.
- Sumiyoshi, K., S. Yamada, & H. Suzuki, 2007a, *Astrophys. J.* **667**, 383.
- Sumiyoshi, K., S. Yamada, & H. Suzuki, 2007b, *Astrophys. J.* **688**, 1176.
- Suwa, Y., Kotake, K., Takiwaki, T., Whitehouse, S.C., Liebend—rfer, M., & Sato, K. 2010, *Publ. Astron. Soc. J.*, 62, 49
- Swesty, F.D. & E.S. Myra, 2009, *Astrophys. J. Suppl.* **181**, 1.
- Takiwaki, T. & K. Kotake, 2011, *Astrophys. J.* **743**, 30.
- Takiwaki, T., K. Kotake, & Y. Suwa, 2012, *Astrophys. J.* **749**, 98.
- Thielemann, F.-K., Nomoto, K., & M. Hashimoto, 1996, *Astrophys. J.* **460**, 408.
- Thompson, T.A., A. Burrows, & P.A. Pinto, 2003, *Astrophys. J.* **592**, 434.
- Thompson, T.A., E. Quataert, & A. Burrows, 2005, *Astrophys. J.* **620**, 861.
- Tubbs, D.L. & D. N. Schramm, 1975, *Astrophys. J.* **201**, 467.
- Symbalisty, E. M. D. 1984, *Astrophys. J.* , **285**, 729.
- Ugliano, M., H.-T. Janka, A. Marek, & A. Arcones., 2012, submitted to *Astrophys. J.* (arXiv:1205.3657).
- Utrobin, V.P. & N.N. Chugai, 2009, *Astron. Astrophys.* **506**, 829.
- Weaver, T.A., G.B. Zimmerman, & S.E. Woosley, 1978, *Astrophys. J.* **225**, 1021.
- Weaver, T. A. & S.E. Woosley, 1993, *Phys. Repts.* **227**, 65.
- Weinberg, N.N. & E. Quataert, 2008, *Mon. Not. R. Astron. Soc.* **387**, L64.
- Wilson, J.R., 1971, *Astrophys. J.* **163**, 209.
- Wilson, J.R., 1985, in *Numerical Astrophysics*, ed. J. M. Centrella, J. M. Leblanc, & R. L. Bowers, p. 422.
- Wongwathanarat, A., H.-T. Janka, & E. Müller, 2010, *Astrophys. J.* **725**, L106.
- Woosley, S.E. & T.A. Weaver, 1986, *Ann. Rev. Astron. Astrophys.* **24**, 205.
- Woosley, S.E. & T.A. Weaver, 1995, *Astrophys. J. Suppl.* **101**, 181.
- Woosley, S.E., A. Heger, & T.A. Weaver, 2002, *Rev. Mod. Phys.* **74**, 1015.
- Woosley, S.E. & J.S. Bloom, 2006, *Annual Rev. Astron. Astrophys.* **44**, 507.
- Yahil, A., 1983, *Astrophys. J.* **265**, 1047.
- Yamasaki, T. & S. Yamada, 2007, *Astrophys. J.* **656**, 1019.
- Yamasaki, T. & T. Foglizzo, 2008, *Astrophys. J.* **679**, 607.

## FIGURES

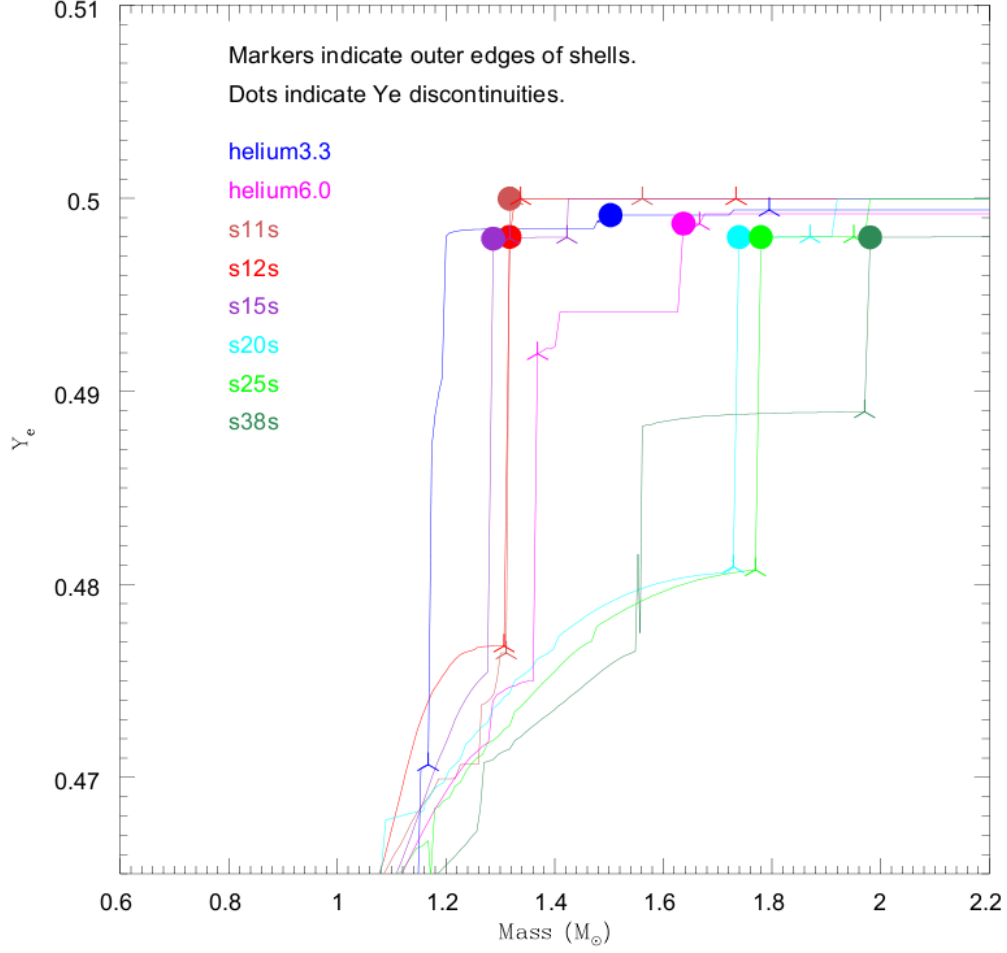


FIG. 1 The electron fraction,  $Y_e$ , versus enclosed mass for a suite of massive-star progenitor models from Woosley & Weaver (1995) (“sXXs”) and Nomoto & Hashimoto (1988 – “heliumX” models). The numbers given (the “X”s in this caption) denote either the ZAMS masses or the helium-core masses. The dots indicate  $Y_e$  discontinuities and the three-pointed markers indicate the boundaries of fossil burning shells. The outer edges of the iron cores are well-marked by the large circular colored dots. Note that they are positioned from  $\sim 1.25 M_\odot$  to  $\sim 2.0 M_\odot$  and are roughly in order of progenitor mass. See text for discussion.

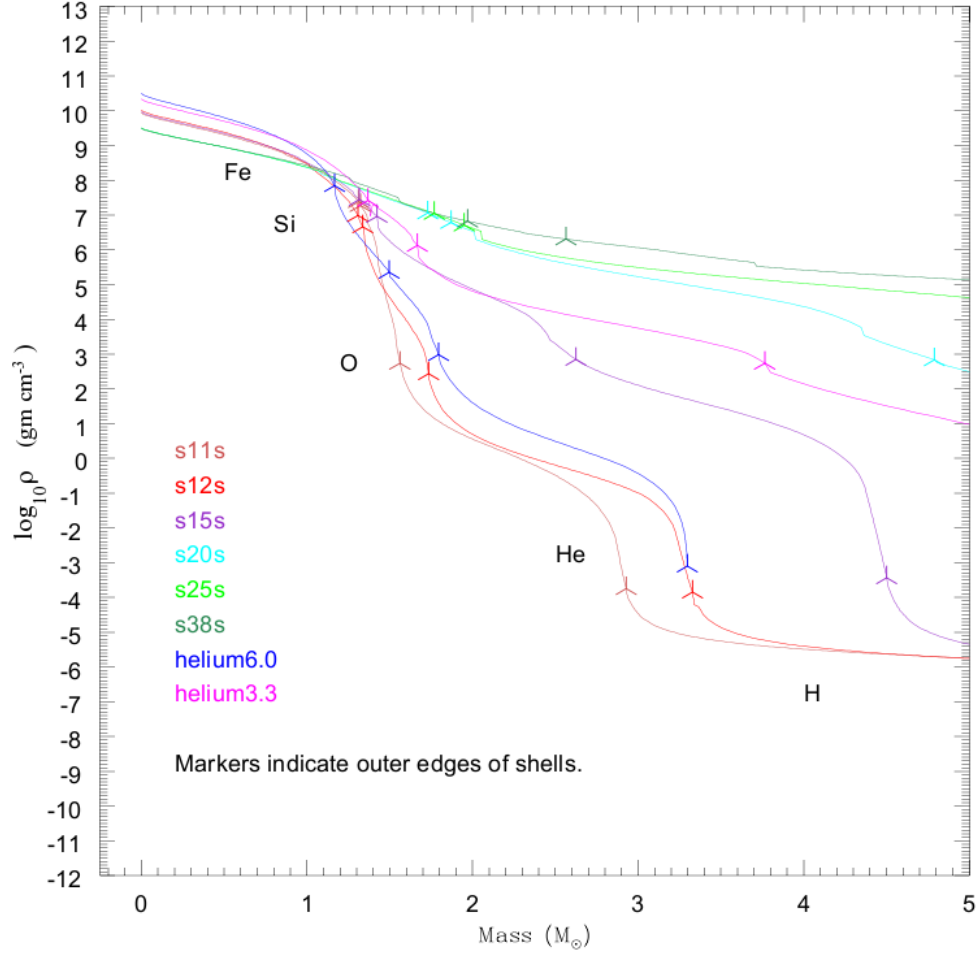


FIG. 2 Similar to Figure 1, but depicting the logarithm of the mass density ( $\rho$ , in  $\text{gm cm}^{-3}$ ) versus interior mass (in solar masses) for various initial progenitor masses. Note that the lower-mass progenitors have steeper slopes, and that these profiles translate into more quickly dropping mass accretion rates ( $\dot{M}$ ) through the stalled shock after bounce.

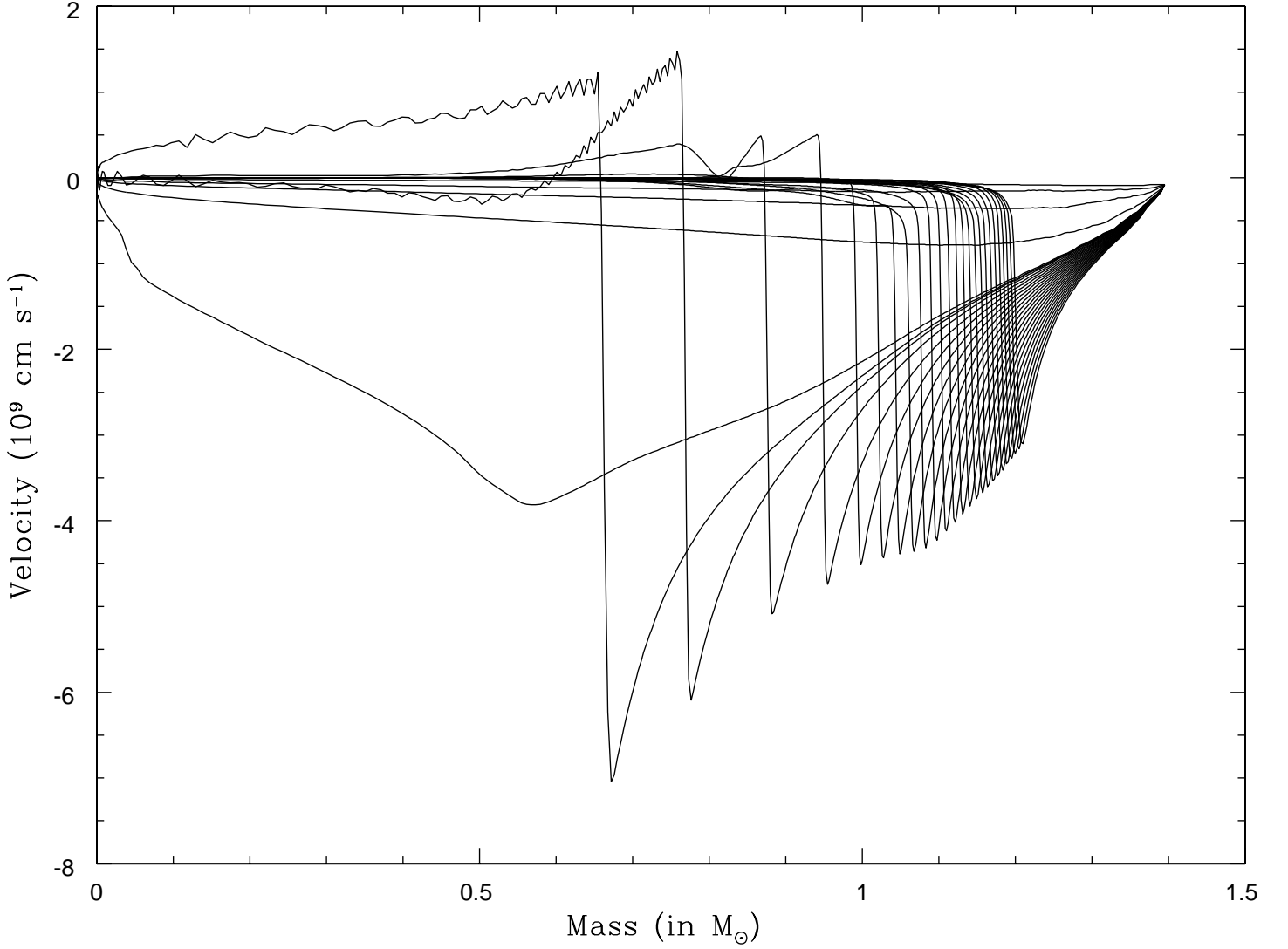


FIG. 3 The velocity (in  $10^9 \text{ cm s}^{-1}$ ) versus interior mass (in solar masses) at various pre- and post-bounce times. The shock wave, when present, is clearly indicated by the vertical drop, and is seen only for the post-bounce times. Within  $\sim 20$  milliseconds of bounce, the shock wave has stalled into accretion and post-shock speeds go negative. Reviving this structure is the goal of modern core-collapse supernova theory. Note the line without the shock that changes slope in the middle. This transition in slope near  $\sim 0.6 M_{\odot}$  marks the edge of the homologous core a few milliseconds before bounce. Exterior to this minimum is the supersonic mantle whose maximum infall speed can reach  $\sim 80,000 \text{ km s}^{-1}$ . The  $11\text{-}M_{\odot}$  progenitor model from Woosley & Weaver (1995) was used for this Figure, as well as for Figures 4, 6, 8, & 9. (Taken from numerical data generated in Thompson, Burrows, & Pinto 2003.)

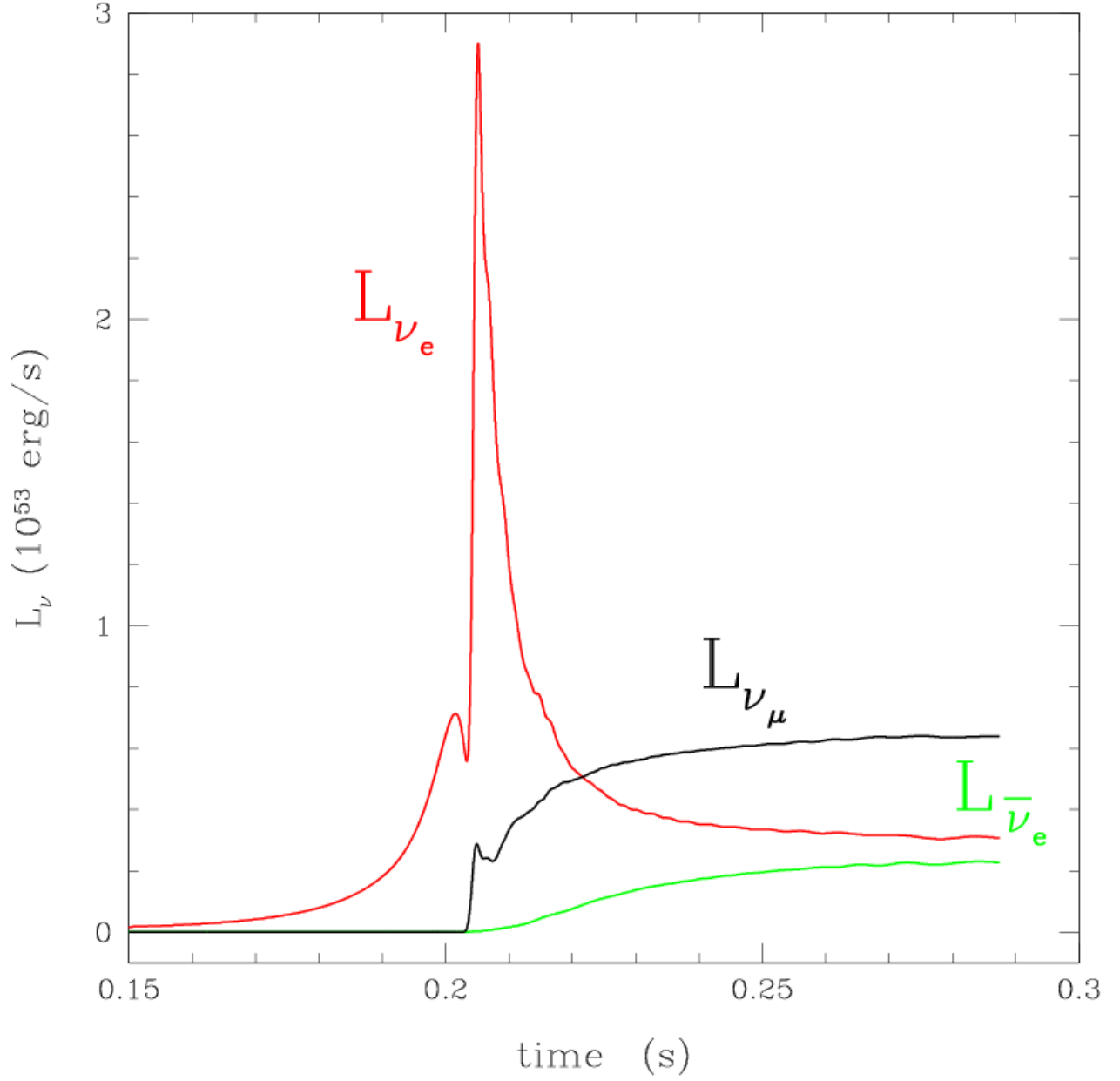


FIG. 4 The luminosity (in units of  $10^{53} \text{ ergs s}^{-1}$ ) at infinity of the  $\nu_e$ ,  $\bar{\nu}_e$ , and, collectively, the  $\nu_\mu$ ,  $\bar{\nu}_\mu$ ,  $\nu_\tau$ , and  $\bar{\nu}_\tau$  neutrinos, versus time (in seconds) around bounce. The  $\nu_e$  breakout burst is clearly seen. After shock breakout, the temperatures are sufficient to generate the other species in quantity. Generally, the non-electron types carry away  $\sim 50\%$  of the total, with the  $\nu_e$ s and  $\bar{\nu}_e$ s sharing the rest. (Plot taken from Thompson, Burrows, & Pinto 2003.)



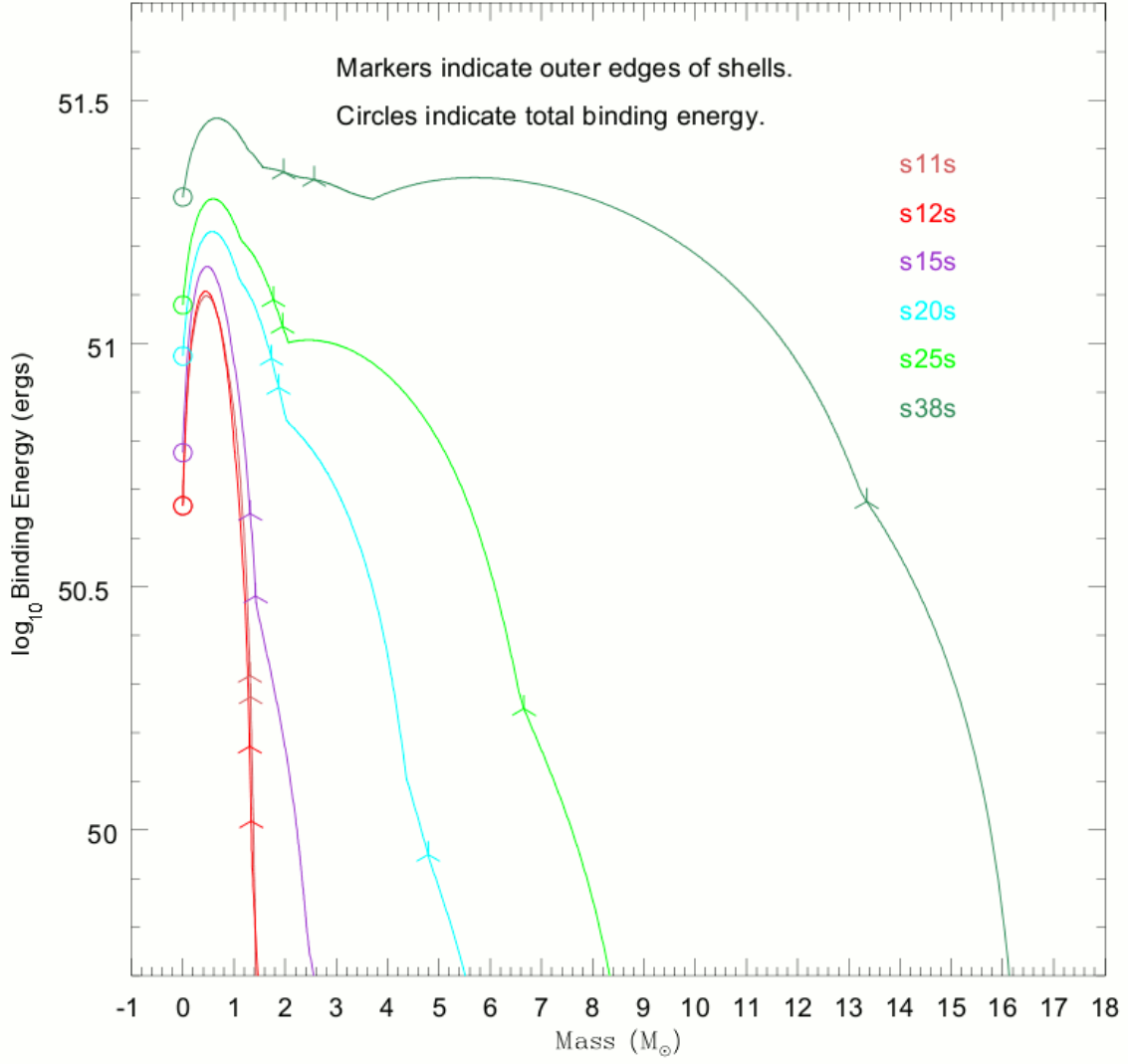


FIG. 5 The logarithm base ten of the gravitational binding energy (in ergs, including the thermal energy) of the shells in various progenitor stars (see Figure 1) exterior to the interior mass coordinate (in  $M_{\odot}$ ) shown on the abscissa. These are the approximate energies that the supernova blast must overcome to eject the stellar shells exterior to a given residual neutron star or black hole mass. Note that the more massive the progenitor the greater the binding energy cost for a given baryon mass left behind.

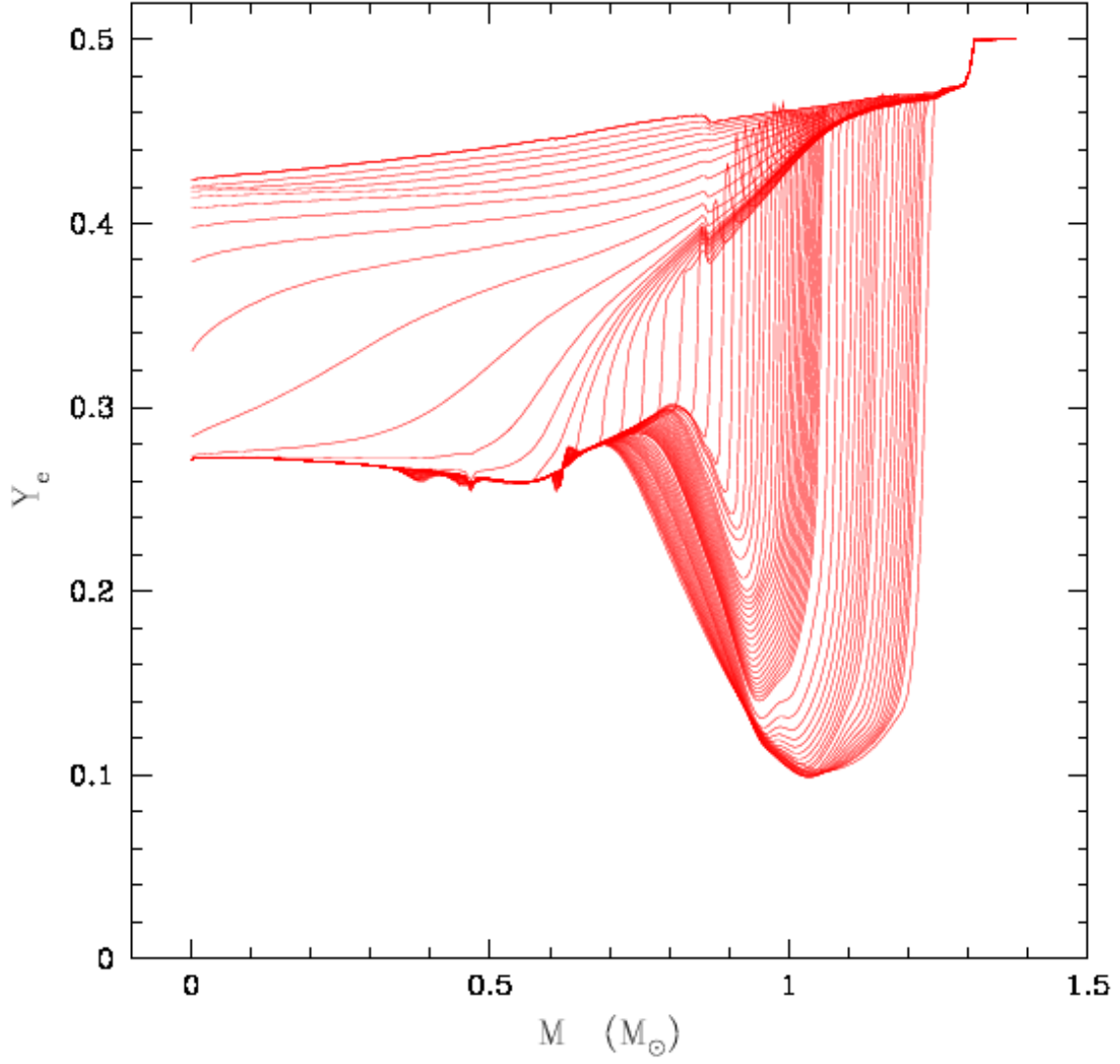


FIG. 6 Snapshots of  $Y_e$  versus interior mass (in solar masses) profiles before and just after bounce. Capture decreases  $Y_e$  on infall, but lepton number is soon trapped in the interior. After bounce, the outward progress of the shock wave liberates  $\nu_e$  neutrinos, creating a trough in  $Y_e$  interior to the shock, but exterior to the opaque core. The shock wave resides just rightward of the steep drop in  $Y_e$  on the right. The numerical data for this  $11 M_\odot$  progenitor model run were taken from Thompson, Burrows, & Pinto (2003).

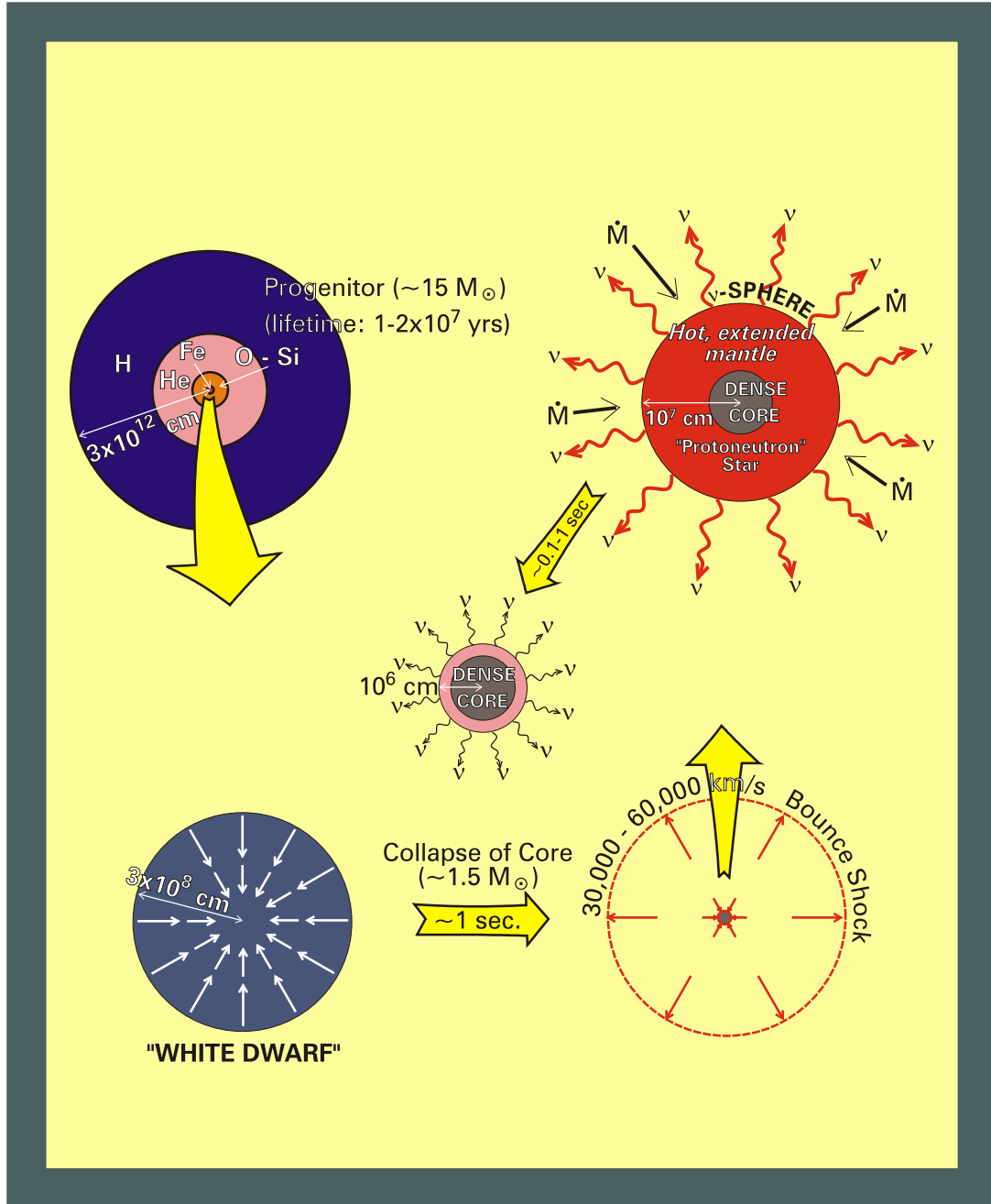


FIG. 7 A storyboard of the evolution of the core of the “onion-skin” structure into the radiating proto-neutron star. See text for a discussion.

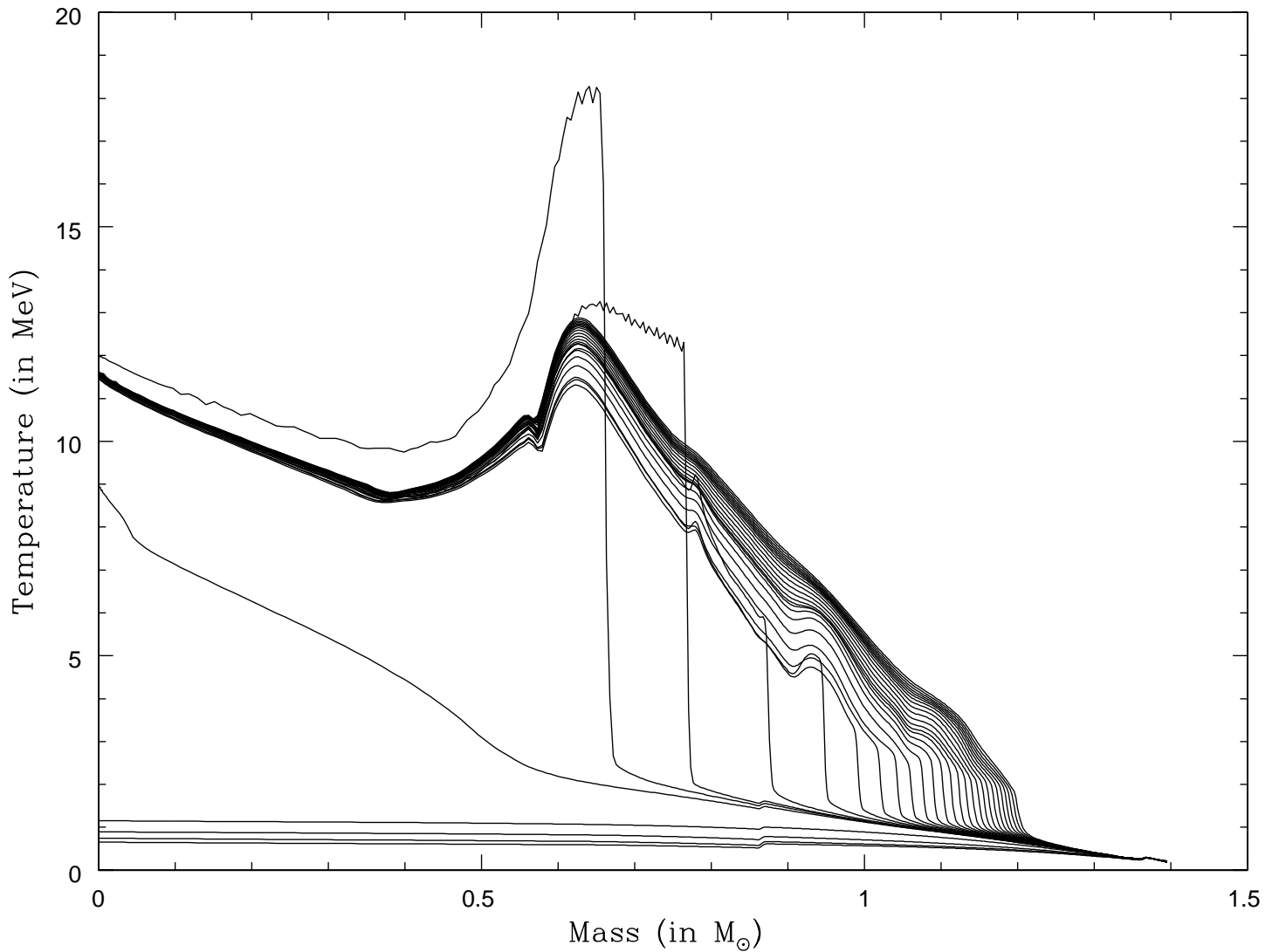


FIG. 8 Temperature (in MeV) versus interior mass (in solar masses) at various times before and just after bounce. The shock is depicted by the vertical drop in temperature and propagates out in mass as (and after) it stalls into accretion. Initial post-bounce central temperatures are  $\sim 10$  MeV and the peak temperature just before shock breakout can exceed 20 MeV, but soon falls. The various neutrinospheres after  $\sim 20$ – $100$  milliseconds after bounce are at  $\sim 1.0$ – $1.1 M_{\odot}$ . (Numerical data taken from Thompson, Burrows, & Pinto (2003).)

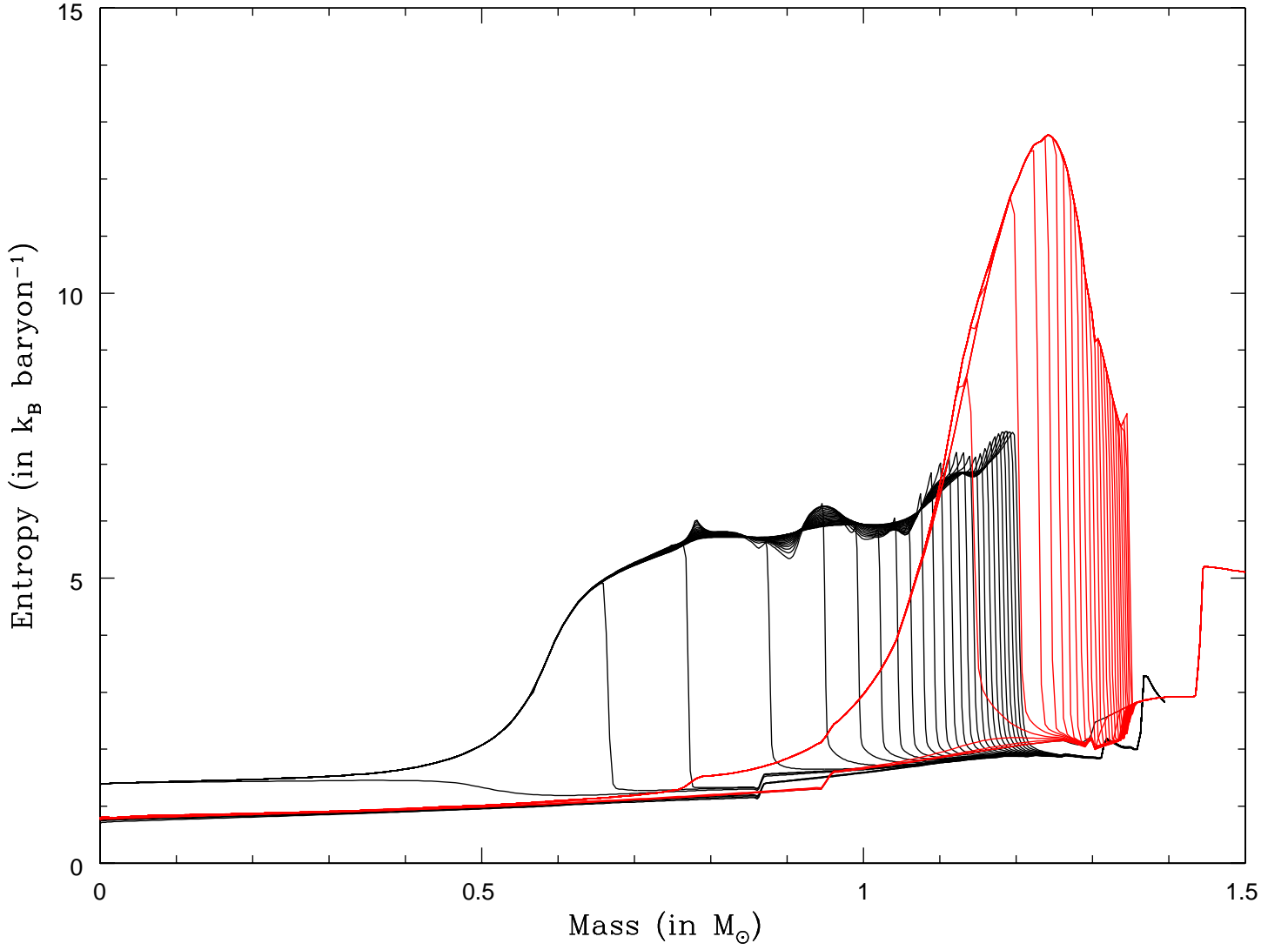


FIG. 9 Similar to Figure 8, but for entropy (in  $k_B$  per baryon) versus interior mass (in solar masses). The black curves depict the evolution of profiles using realistic neutrino transport and stopping  $\sim 10$  milliseconds after bounce, while the red curves depict the corresponding developments when neutrino physics is turned off. Note that the red curves extend further in mass and reach much higher early mantle entropies. See text for discussion. (Numerical data taken from Thompson, Burrows, & Pinto (2003).)

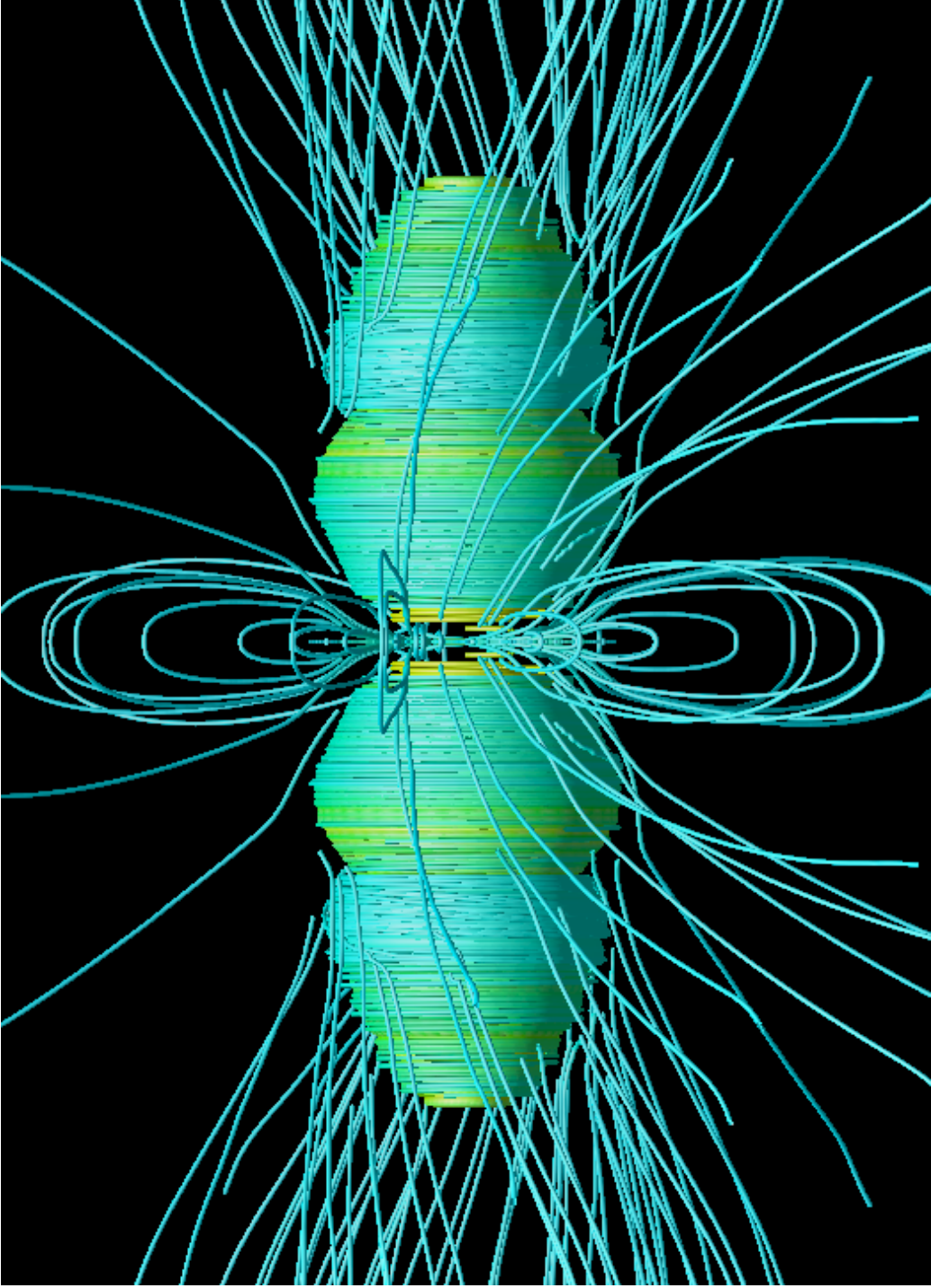


FIG. 10 An early snapshot during the bipolar explosion of the mantle of a rapidly-rotating core. Depicted are representative magnetic field lines. The scale is 2000 km from top to bottom. The extremely twisted lines are just interior to the shock wave being driven out by magnetic pressure generated within 200 milliseconds of bounce in a “2.5”-dimensional magneto-radiation-hydrodynamic calculation conducted by Burrows et al. (2007d). The progenitor employed for this calculation was the 15- $M_{\odot}$  model of Heger et al. (2005).



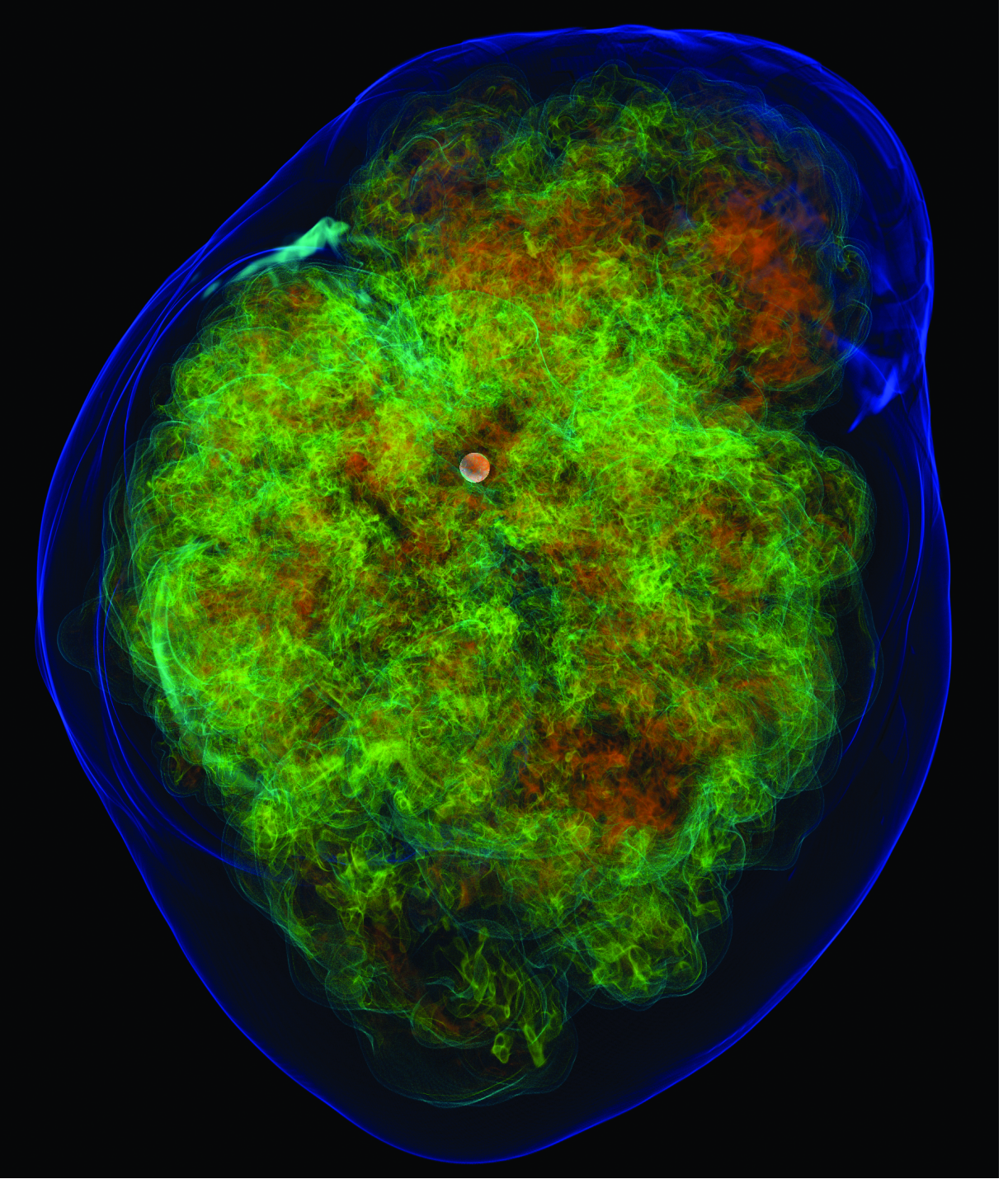


FIG. 11 The debris field generated in a 3D neutrino-driven explosion approximately 200 milliseconds after its onset. The scale from top to bottom is 1000 km. The blue exterior is a rendering of the shock wave, the colored interior is a volume-rendering of the entropy of the ejecta, and the sphere in the center is the newly-born neutron star. (Numerical data taken from Nordhaus et al. (2010) and the 15- $M_{\odot}$  progenitor from Woosley & Weaver 1995 was used.)



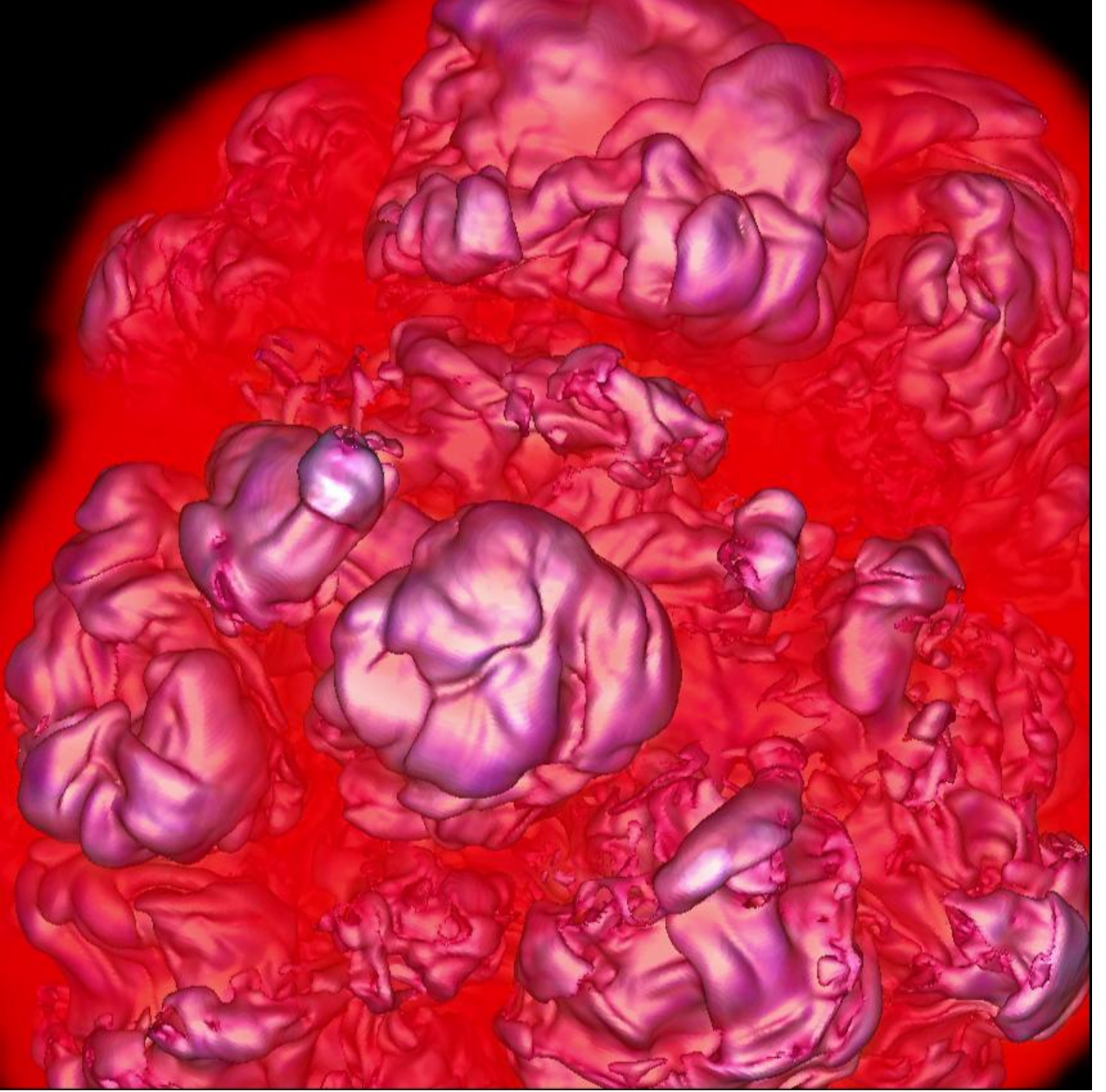


FIG. 12 A different rendering of the 3D neutrino-driven explosion shown in Figure 11, but approximately 25 milliseconds after its onset. The scale from top to bottom is  $\sim 500$  km. The prominent bubble structures in magenta are isoentropy surfaces and are provided to highlight the neutrino-heated bubbles that seem to be generic in current 3D simulations. The bounding shock is not shown. The red colored interior (between the bubbles) is an experimental (only partially successful) volume-rendering of the density. (Numerical data taken from Nordhaus et al. (2010) and the  $15\text{-}M_{\odot}$  progenitor from Woosley & Weaver 1995 was used.)